4-5-2014

Measuring Viability of the Red-Tide Dinoflagellate Lingulodinium polyedra Following Treatment with Ultraviolet (UV) Light

Scott Riley
Nova Southeastern University, scotrile@nova.edu

NOVA SOUTHEASTERN UNIVERSITY OCEANOGRAPHIC CENTER

Measuring Viability of the Red-tide Dinoflagellate *Lingulodinium polyedra* Following Treatment with Ultraviolet (UV) Light

By
Scott Riley

Submitted to the Faculty of
Nova Southeastern University Oceanographic Center
in partial fulfillment of the requirements for
the degree of Master of Science with a specialty in:

Coastal Zone Management

4/5/2014
Nova Southeastern University

Thesis of Measuring Viability of the Red-tide Dinoflagellate *Lingulodinium polyedra* Following Treatment with Ultraviolet (UV) Light

Submitted in Partial Fulfillment of the Requirements for the Degree of

Masters of Science:

Coastal Zone Management

Nova Southeastern University
Oceanographic Center

April, 2014

Approved:

Thesis Committee

Major Professor: _____
Clarice Yentsch, Ph.D.

Committee Member: _____
Jose Victor Lopez, Ph.D.

Committee Member: _____
Matt First, Ph.D.

Abstract:

Harmful algae blooms (HABs) have caused millions dollars in annual losses to the aquaculture industry, inhibited beach recreation, and have threatened marine and human health. HABs and red tides can develop suddenly and their frequency, geographic range, and intensity have increased over the past decade. A possible source for spreading and seeding new areas expanding the geographic range of HABs is ballast water. The process of ballast water discharge has been identified as a primary vector for the translocation of non-indigenous species (NIS) and invasive species. National and international efforts are currently underway to address the impact of NIS and invasive species. Policy is being developed detailing stringent rules to kill, remove, or otherwise inactive organisms in ballast water prior to or upon discharge. Currently, vendors are developing technologies to treat ballast water and U.S. and international facilities are testing these technologies to verify their efficacy. Ultraviolet (UV) radiation is commonly employed in ballast water treatment technologies. Previous studies have shown that UV light is effective for disinfecting drinking water, but the response of non-pathogenic and marine organisms is largely unknown.

The purpose of this research was to measure the viability of the durable red-tide forming dinoflagellate, *Lingulodinium polyedra* following UV treatment. Two methods were used to measure the viability signal; manual epifluorescence microscopy with correlated viability stains and Pulse Amplitude Modulated (PAM) fluorometry to measure the physiological state of the organism following UV treatment. The number of cysts was also enumerated. The results showed that there was a significant decrease in the number of living *L. polyedra* cells following a UV treatment of more than 100 mWs cm^{-2}. The results also have showed a significant increase in the number of *L. polyedra* cysts following UV treatment as low as 50 mWs cm^{-2}.

***Keywords*:** Ballast water, Pulse Amplitude Modulated (PAM) fluorometry, fluence, cysts

Acknowledgements:

I would like to deeply thank my advisor, Dr. Clarice Yentsch for her support and professional guidance during this research project. I would like to thank my committee members, Dr. Jose Lopez and Dr. Matt First for their knowledge and direction. I greatly appreciate the comments and suggestions by Stephanie Robbins-Wamsley. I would also like to thank Diane Lysogorski, Section Head of NRL Code 6136 and Director of the Center for Corrosion Science and Engineering, Key West, Florida for allowing me to conduct my research on the property and use the laboratory equipment to fulfill the research needs during non-work hours. Finally, I would like to thank my wife, Lisa Riley and my two children Hayden and Grace Riley for their unconditional love and support during this research effort.

Table of Contents

I. Introduction

Harmful algae blooms (HABs, e.g. 'red tides') are natural phytoplankton blooms that cause millions of dollars in annual losses to the aquaculture industry (Alonso-Rodriguez R. and F. Paez-Osuna 2003), threaten marine mammals and human health (Anderson 1997), and inhibit beach recreation (Backer et al. 2003). HABs are triggered in localized areas that are rich in inorganic nutrients and occur more frequently in the summer months when days are longer and water temperatures are the highest (Omand et al. 2011). Coastal advection (tidal currents and stirring, internal tides, and internal wave induced circulation) has also been linked to triggering phytoplankton blooms, which can make predicting their occurrence extremely difficult (Cloren J. E. and R. Dufford. 2003; Lennert-Cody C.E. and P.J.S. Franks 1999).

HABs can develop suddenly. Most of the red tide dinoflagellates form dormant cysts that can survive in the oceans sediment for numerous years (Pfiester L.A. and D.M. Anderson 1987). Under appropriate environmental conditions, the resuspended cysts germinate to produce red tides and HABs. The process of encystment is characterized as a mode of escaping unfavorable or adverse conditions.

The frequency of HABs, geographic range and intensity have increased since the 1970s and appear to be stimulated by nutrient discharges in domestic, industrial, and agricultural wastes (Lam C.W.Y and K.C. Ho 1989). Climate changes combined with nutrient runoff could further increase the frequency of HABs in years to come (Camacho et al. 2007). A possible source for seeding new areas expanding the geographic range of HABs is ballast water.

Nearly all commercial and military ships and some leisure vessels carry ballast water onboard. The ballast water is stored in tanks aboard a ship and serves a variety of purposes: management of the ship's trim and list, providing stability during transit, and maintaining draft during the on-loading and off-loading of cargo or during changing weather conditions. The ballast water volume for any given ship can be tremendous at times with volumes reaching thousands of metric tons. Frequently, ship's tanks will be ballasted in one port and de-ballasted in another. This process has been identified as a primary vector for the translocation of non-indigenous species (NIS) and invasive species. This transporting process of NIS and invasive species has not only caused significant ecological and financial problems in the United States (US) and worldwide, but it may be contributing to the spread of toxic dinoflagellates and their cysts to nonnative regions (Camacho et al. 2007).

National and International efforts are currently underway to mitigate the movement and impact of NIS and Invasive species. The International Maritime Organization (IMO), which governs international maritime law, ratified the International Convention for the Control and Management of Ships' Ballast Water and Sediments (IMO 2004),

which sets limits on concentrations of viable organisms in order to reduce the transport and transfer of NIS by ships' ballast water. The US Environmental Protection Agency (EPA) in collaboration with US Coast Guard (USCG) (Environmental Standards Division, Washington DC) and US Naval Research Laboratory (Center for Corrosion Science and Engineering, Washington DC) developed similar standards by creating the Generic Protocol for the Verification of Ballast Water Treatment Technology through the Environmental Technology Verification (ETV) program. Both documents outline stringent standards specifying the maximum number of viable organisms allowed in a vessel's discharged ballast water resulting in the need for on-board ballast water management systems (BMWS). These BMWS must kill, remove or otherwise inactive organisms prior to or upon discharge of ballast water. Commercial vendors are currently developing technologies to treat ballast water to concur with the set standards. These BMWS must also undergo verification testing outlined by the IMO and EPA/USCG prior to being employed on a vessel. The verification of BWMS is currently taking place at multiple US facilities and international sites around the world.

Ultraviolet (UV) light radiation is commonly employed in BWMS as a treatment approach to kill or otherwise inactivate organisms suspended in a fluid prior to discharge of ballast water (Tsolaki E. and E. Diamadopoulos 2010). The mechanics of inactivation involves UV light being absorbed by DNA or RNA pyrimidine bases (thymine or cytosine in DNA and uracil or cytosine in RNA) resulting in a photochemical reaction where a chemical dimer forms between the two bases. This dimer inhibits the formation of new DNA (or RNA) chains during the process of mitosis and gene expression thus resulting in an inability to replicate (Bolton J.R. and K.G. Linden 2003). Studies have shown that UV light is very effective for disinfection of drinking water and wastewater (Meulemans 1987; Von Sonntag C. and H.P. Schuchmann 1992; Jacangelo et al. 1995), however, the response of non-pathogenic and marine organisms to UV light is largely unknown. IMO and EPA/USCG guidelines categorize organisms by size classes based on minimum dimensions: ≥ 50 μm (nominally zooplankton), ≥ 10 μm and < 50 μm (nominally protists), and < 10 μm (nominally microalgae and bacteria). Facilities that perform verification testing of BWMS examine the respond of the assemblage of organisms in each size class, and the organisms that are tested are indigenous to region of the test facility.

Lingulodinium polyedrum (Stein) Dodge is a red-tide forming dinoflagellate that has been linked to the production of yessotoxin (Yasumoto T. and A. Takizawa 1997). Mussels, scallops, clams, and gastropods contain this toxin, which can lead to Diarrhetic shellfish poison (DSP) (Camacho et al. 2007). *Lingulodinium polyedra* is a sophisticated organism with three main processes that comprise its life cycle: vegetative reproduction, formation of ecdysal stages, and sexual reproduction (Lewis, J. and R. Hallet 1997). *L. polyedra* can morphologically transition from a motile planozygate to a mature

hypnozygote within 10-20 minutes (Kokinos J. P. and D.M. Anderson 1995) triggered by an ambient change or adverse conditions. When favorable conditions return, cysts can germinate within 24 hours (Balzer 1996). *L. polyedra* also produces concentrations of melatonin, which functions as a mediator regulating the organism's circadian rhythm (Balzer 1996). Research has shown that the formation of cysts by *L. polyedra* is not only a protective mechanism, but also a photoperiodic response as melatonin provides the internal signal for darkness as encystment occurs with shortening of days associated the decrease in temperature resulting in resting cyst formation during winter months (Balzer I. and R. Hardeland 1991; Balzer 1996). Finally, *L. polyedra* has the ability to excrete ultraviolet-absorbing compounds known as mycosporine-like amino acids (MAA). Experiments have shown that excreted metabolites by the organism contributed to both the particulate and dissolved organic pools with maximum ultraviolet (UV) absorption at 360 nm allowing the organism to protect itself from UV-B radiation (M. Vernet and K. Whitehead 1996). The complexity of *L. polyedra* life cycle, rapidity of encystment and excystment, sensitivity to ambient conditions mediated by internal signal, and use defense mechanisms characterizes *L. polyedra* as durable organism with the ability to survive.

The purpose of this research was to test the hypothesis that increased exposure to UV treatment will kill or inactivate the durable organism, *L. polyedra.* The viability of the organism was measured using multiple techniques (epifluorescence microscopy with viable stains and Pulse Amplitude Modulated [PAM] fluorometry) and the number of cysts was enumerated at set time points. Two UV instruments were used to treat samples allowing for a wide range of UV doses to be evaluated. The research was conducted at the Naval Research Laboratory in Key West, Florida (NRL-KW). NRL-KW is a laboratory that conducts corrosion research for the United States Navy as well as biological research on ballast water and biofouling. The facility provided all of the necessary tools and equipment (e.g., incubators, microscopes, biological safety cabinets, etc.) to complete this research project.

II. Objectives

The objective of this research was to examine the response of *Lingulodinium polyedra* to UV treatment at various dose treatments. Viability was measured using multiple techniques at set times following treatment. Cysts were enumerated at each of the set time points to further assess the organism response. Collected data from each experimental trial was generated and assessed to test the stated hypothesis.

III. Hypothesis

To compare the viability of *Lingulodinium polyedra* among UV treatments, the following hypotheses were evaluated:

• Ho: There is no significant difference in measured viability of *L. polyedra* between UV treatments.

• Ha: There is a significant difference in measured viability of *L.polyedra* between the UV treatments.

IV. Methods and Materials

1. Experimental Location

Experiments were performed from July of 2013 until February of 2014 at the Naval Research Laboratory (NRL-KW) located on Fleming Key on Trumbo Point Annex, United States Naval base, adjacent to the island of Key West. Corrosion science and biological research on ballast water and biofouling are examples of topics investigated at the laboratory. Experiments were conducted in a biological laboratory, following standard protocols. Permission to conduct this research was granted by the NRL-KW Section Head, Diane Lysogorski, at the facility during non-working hours.

2. Cultured *Lingulodinium polyedra*

Cultures of the obligate autotrophic dinoflagellate *Lingulodinium polyedra* were purchased from the National Center for Marine Algae and Microbiota, Bigelow Laboratory for Ocean Sciences (NCMA, Bigelow, ME). Cultures were incubated in a Percival Incubator (Model # I-66LL, Perry, Iowa) at a 12:12 light: dark regime with a light intensity of 5000 lux. The cultures were kept at 20°C and were monitored weekly using the PAM fluorometer (see below for PAM fluorometer methods; data not shown). Cultures of *L. polyedra* were initially maintained by a removing 2 mL aliquot from a well-mixed culture tube and dispensing into 8 mL of autoclaved (121°C and 18 psi for 45 min) 0.22 μm filtered seawater enriched with nutrients (i.e. sterile medium; Guillard R.R.L. and Ryther J.H. 1962); cultures were transferred every 3 weeks using sterile techniques. For the purpose of increasing culture volume, large stock cultures were created and maintained by removing 50 mL of well mixed culture and dispensing into 350 mL of sterile medium. These large stock culture transfers occurred every 4 weeks using sterile techniques.

3. Ultraviolet (UV) Radiation Instrumentation

Two types of instrumentation were used to deliver UV radiation to samples of *Lingulodinium polyedra*: UV Crosslinker and UV Collimated Beam. Standardized methods were developed for each bench-top apparatus which allowed for reliable and repeatable UV treatments during experimentation.

3.1. UV Crosslinker

The Ultraviolet Products (UVP) CL-1000 Ultraviolet Crosslinker (product # UVP95017401; Fisher Scientific, Suwannee, GA.) is a tabletop chamber unit which uses a 254 nm wavelength, low-pressure mercury blub (Figure 1). The control system has a maximum UV energy exposure setting of 999,900 micro-joules per cm^2 ($\mu J\ cm^{-2}$), which relates to a maximum UV time exposure setting of 999.9 minutes. This is controlled by a touch screen interface. Even though the Crosslinker has an internal sensor that continually measures the fluence, a radiometer (Ultraviolet Products (UVP) Inc., product # UVP97001601: Fisher Scientific, Suwannee, GA.) was used to verify and record the fluence prior to each experiment (Figure 1; see Appendix A for UV conversions using radiometer to measure fluence of crosslinker). Well-mixed suspensions of *L. polyedra* samples (30 mL) were dispensed into sterile, plastic Petri dishes (10 cm diameter; 1.5 cm deep) with the lids removed. The water depth was low (5 mm) to minimize the attenuation of UV radiation, and an opaque cylinder cut from polyvinyl chloride piping (5 cm in height) was placed on the rim of the Petri dish so the incident light upon the sample was directed only from above to avoid the scattering of the light source. Because fluence is constant, the pre-determined dose was controlled by exposure time. See Table 1 for the required exposure times for each UV treatment. This exposure time was controlled by the touch screen interface of the crosslinker and was also monitored using a stopwatch. The experiments using the crosslinker account for the high end treatments (0, 100, 300, and 500 mWs cm^{-2}) as a low dose could not be attained due to the parameters of the instrument apparatus (i.e. low measureable exposure times).

Table 1: Required exposure time for each dose of UV treatment using the crosslinker.

UV Treatment Dose (mWs cm^{-2})	Exposure Time (sec)
500	**124**
300	**75**
100	**25**
0	**124***

*** The control sample was placed within UV crosslinker chamber and the exposure time was measured for 500 mWs cm^{-2}, but the bulb was not ignited and the sample did not receive UV treatment.**

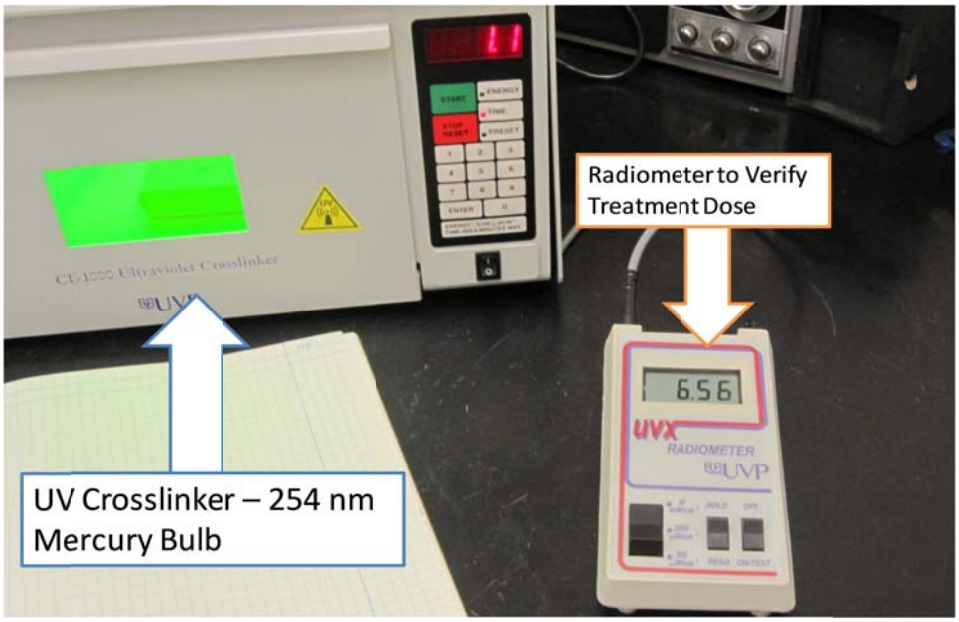

Figure 1: Left: Ultraviolet Crosslinker (Ultra-Violet Products (UVP) CL-1000) with 254 nm low-pressure mercury blub. Right: The UVP UVX Radiometer used to verify the fluence prior to treatment.

3.2. UV Collimated Beam

The UV collimated beam (Trojan UV, Inc., Ontario, Canada) delivers an even and measureable dose of UV radiation directly to a sample. The UV housing holds a 254 nm low-pressure mercury bulb and the emitted UV light is directed upon a sample by a collimator. Each well-mixed *L. polyedra* sample (25 mL) was dispensed into glass Petri dishes that were placed upon a stirring plate, which allowed for continuous mixing during treatment. Prior to experimentation, a radiometer was used to verify the fluence for validation of each UV treatment. An overview of the UV collimated beam can be seen in Figure 2. An opaque plate was used to block the UV light and to stop irradiation in-between treatment of samples. To start a treatment, the plate was moved and a stopwatch was used to measure the exact exposure time. The treatment process was stopped by blocking the light with the opaque plate at the end of the required exposure time. See Table 2 for the required exposure times for each UV treatment using the UV collimated beam. The experiments using the UV collimated beam account for the low-end UV treatments (0, 20, 50, 100, and 200 mWs cm^{-2}) as the apparatus is highly sensitive and controllable delivering an exact dose of known UV treatment.

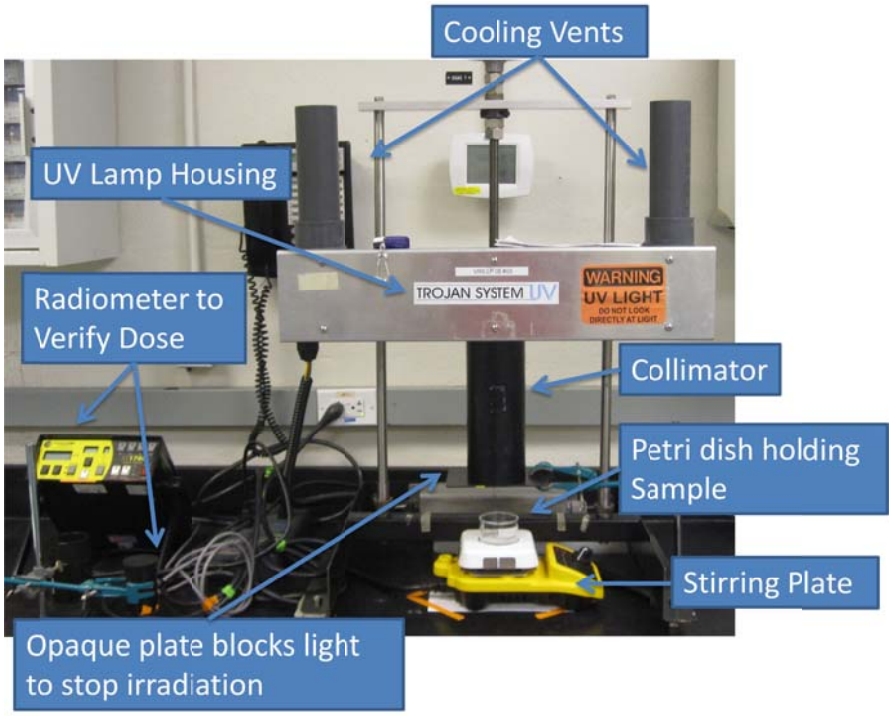

Figure 2: Overview of the UV Collimated Beam (Trojan UV, Inc., Ontario, Canada) apparatus and location of instrumentation.

Table 2: Required exposure time for each dose of UV treatment using the UV collimated beam.

UV Treatment Dose (mWs cm^{-2})	Exposure Time (sec)
200	**1382.18**
100	**691.09**
50	**345.54**
20	**138.22**
0	***1382.18**

*** The control sample was placed on the stirring plate, mixed, and the exposure time was measured for the 200 mWs cm^{-2}, but the opaque plate blocked the UV light and the sample did receive treatment.**

3.2.1. Correction factors - UV Collimated Beam

Incidental irradiation/fluence is a function of a number contributing factors that must be accounted for to obtain an accurate and measurable UV dose. These adjustments required measurements and calculations that were made prior to the treatment of samples. Bolton J.R. and K.G. Linden 2003 standardized these adjustments and their outlined procedures were followed for required correction factors of the UV collimated beam (Appendix B – Excel spreadsheet used for collimated beam correction factors).

- **Reflection Factor -** When the UV light passes through one medium (air) to another (the sample water) where the refractive index changes, a small fraction of the beam is reflected off the interface between the two media. For a standard incident beam, the fraction reflected R is provided by the Frensel Law. For air and water, the mean refraction indices for 200 to 300 nm range are 1.000 and 1.372. So for air and water R = 0.025, and the reflection factor is $1 - R$ which equals 0.975. The value represents the fraction of the UV beam that enters the sample water and was accounted for in calculating the exposure time.

- **Petri Factor -** Because the fluence is slightly varied over the surface of the sample, the Petri factor had to be determined. The Petri factor is the ratio of the average fluence over the area of the Petri dish to the fluence at the center of the Petri dish. This ratio is used to correct the fluence reading at the center of the Petri dish to accurately reflect the average incident fluence over the surface of the sample. The Petri factor was determined by using a radiometer to measure the fluence values at each specified locations using a coordinate map. This map is displayed in Figure 3. The fluence readings at each grey dot were divided by the center fluence reading and the average of these ratios was used in the final calculations.

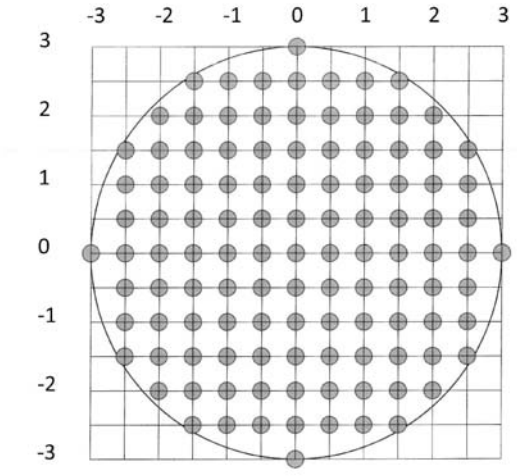

Figure 3: Gridded map used to determine the Petri factor.

- **Water Factor (absorption)** – Because the sample water absorbs UV light, there is a decrease in fluence as the beam passes through the sample water. The Water Factor is defined as

$$\text{Water Factor} = \frac{1 - 10^{-\text{al}}}{\text{al}\ln(10)}$$

Where α =decadic absorption coefficient (cm^{-1}) and l = vertical path length (cm) of the sample water in the Petri dish.

- **Divergence Factor** – Because there is a distance of the UV light to the sample water, the beam is not perfectly collimated and diverges to some extent. This Divergence Factor had to be accounted for and is defined as

$$\text{Divergence Factor} = \frac{L}{(L+l)}$$

L = the distance of the UV lamp to the surface of the sample and l = path length between collimator the surface of the sample.

- **Average Germicidal Fluence -** Finally, the average germicidal fluence rate E'_{avg} (W cm^{-2}) to the sample water is defined as

$E'_{avg} = E_0$ x Petri Factor x Reflection Factor x Water Factor x Divergence Factor

where E_0 equals the fluence reading by the radiometer at the center of the Petri dish and at the same vertical position as the surface of the sample water within the Petri dish. Thus, the given value of E'_{avg} = 15.4 mW cm^{-2} is used to deliver the exact dose control by exposure time (sec).

4. UV Crosslinker Trials – Experimental Approach

An overview of the experimental approach for the UV crosslinker trials is presented in Figure 4. The original sample (150 mL) of *Lingulodinium polyedra* was analyzed to verify the target concentration (1000 – 3000 mL^{-1}) and to check the stability and health of the organism within the sample. This data is not presented. The original sample was then split into 4 well-mixed aliquots (30 mL), each receiving the specified UV treatment; low UV (100 mWs cm^{-2}), medium UV (300 mWs cm^{-2}), high UV (500 mWs cm^{-2}), and control (0 mWs cm^{-2}). Following UV treatment, samples were dispensed into designated Falcon tubes to await analysis. Sample analysis occurred immediately after treatment (T_1), at 24 hours (T_2), and at 3 days (T_3) to measure the change in the viability signal. The samples were incubated under standard light conditions (12:12 Light: Dark), and temperature of 20°C allowing for photo-repair in optimal conditions.

The analysis suite for the UV crosslinker trials required a minimum volume of 10 mL of sample at each analysis time point necessitating 30 mL in the treated sample. An

overview of the sample volume budget is displayed in Figure 5. The PAM fluorometry analysis required 9 mL of sample to collected 3 replicated readings. The epifluorescence microscopy required 1 mL of sample at each analysis time point. Data collect during UV treatment (e.g. exposure time, sample volume, etc.) was recorded on separate data sheets for each trial (See Appendix C).

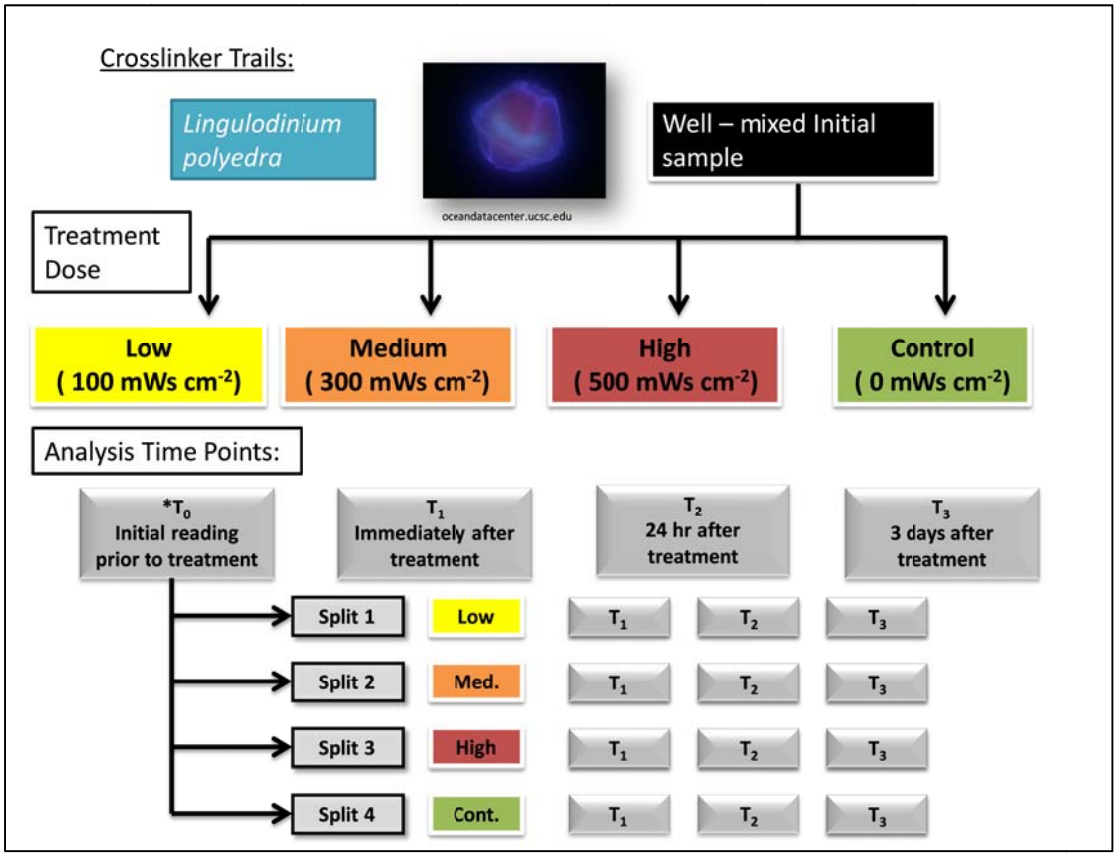

Figure 4: Overview of the experimental approach for the UV crosslinker trials. * Initial readings were used to verify target concentrations (1000 – 3000 mL^{-1}) and physiological status (via PAM fluorometry) of organisms prior to treatment. This data is not presented.

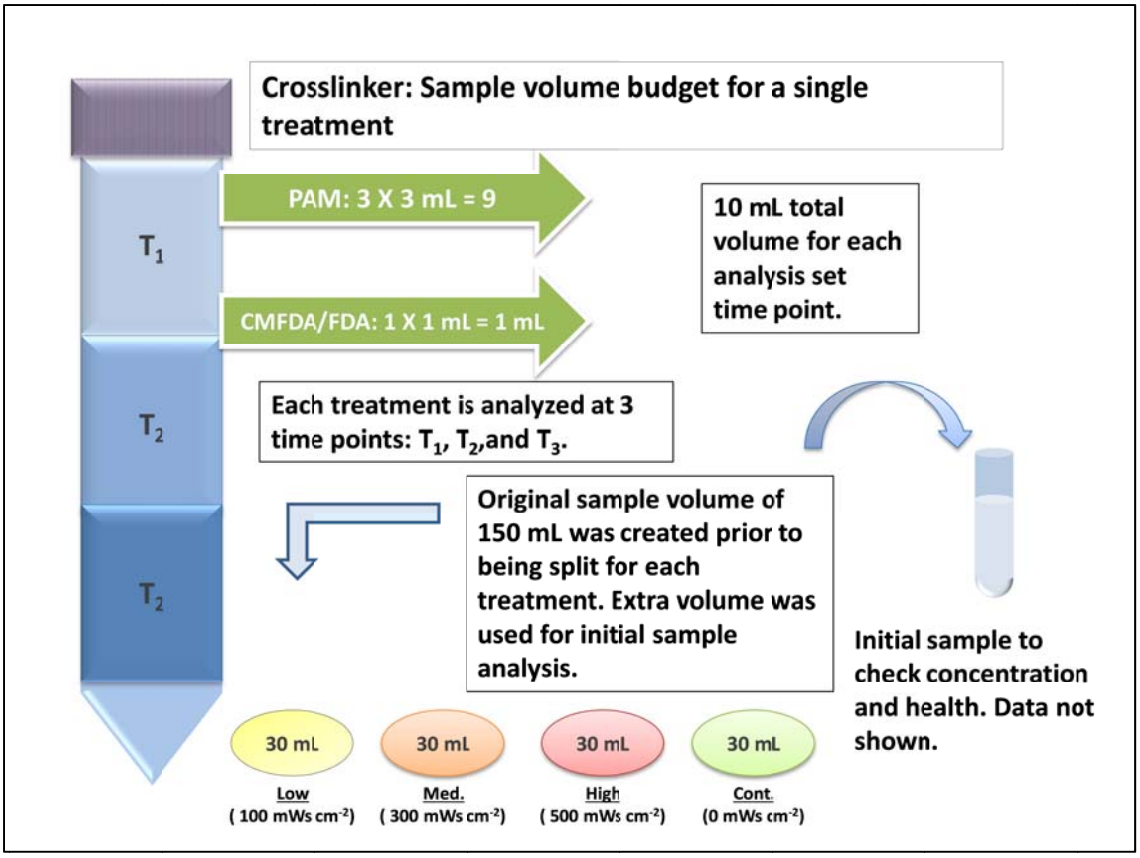

Figure 5: Sample volume allocation for a single treatment during a UV crosslinker trials.

5. UV Collimated Beam Trials – Experimental Approach

The experimental approach for the UV collimated beam was similar to the UV crosslinker approach with some differences for the purpose of examining *Lingulodinium polyedra* response over a longer time period. This extended time period was also to assess if treated *L. polyedra* could recover and/or replicate.

An overview of the experimental approach for the UV collimated beam trials is seen in Figure 6. The original stock sample (200 mL) of *L. polyedra* was analyzed to confirm the target concentration (1000 - 3000 mL^{-1}) and to check the physiological status (health) via PAM fluorometry of the organism within the sample. This data is not presented. The original sample was then split into 5 well-mixed aliquots (25 mL) each receiving a specified UV treatment; low UV (20 mWs cm^{-2}), medium UV (50 mWs cm^{-2}), high UV (100 mWs cm^{-2}), extreme UV (200 mWs cm^{-2}), and control (0 mWs cm^{-2}). After UV treatment, samples were dispensed into individual designated Falcon tubes to await analysis. The set time periods for analysis were immediately following treatment (T_1) at 24 hours (T_2) at 3 days (T_3), at 5 days (T_4), and at 10 days (T_5) to measure the change in the viability signal and to assess replication of the organism. The samples were

incubated under standard light conditions (12:12 Light: Dark), and temperature of 20°C allowing for photo-repair in optimal conditions.

An overview of the sample volume allocation for the UV collimated beam trials is displayed in Figure 7. The analysis suite necessitated a minimum volume of 4 mL from each sample at each analysis time point taken from the total 25 mL volume of the treated sample. The 25 mL volume was required in the correction factors of the UV collimated beam (See Section 3.2.1). The PAM fluorometry analysis required 3 mL of sample to collect a single replicate (the mean of 3 readings) reading and the epifluorescence microscopy required 1 mL of sample at each analysis time point. Data collect during UV treatment (e.g. exposure time, sample volume, etc.) was recorded on separate data sheets for each trial (See Appendix C).

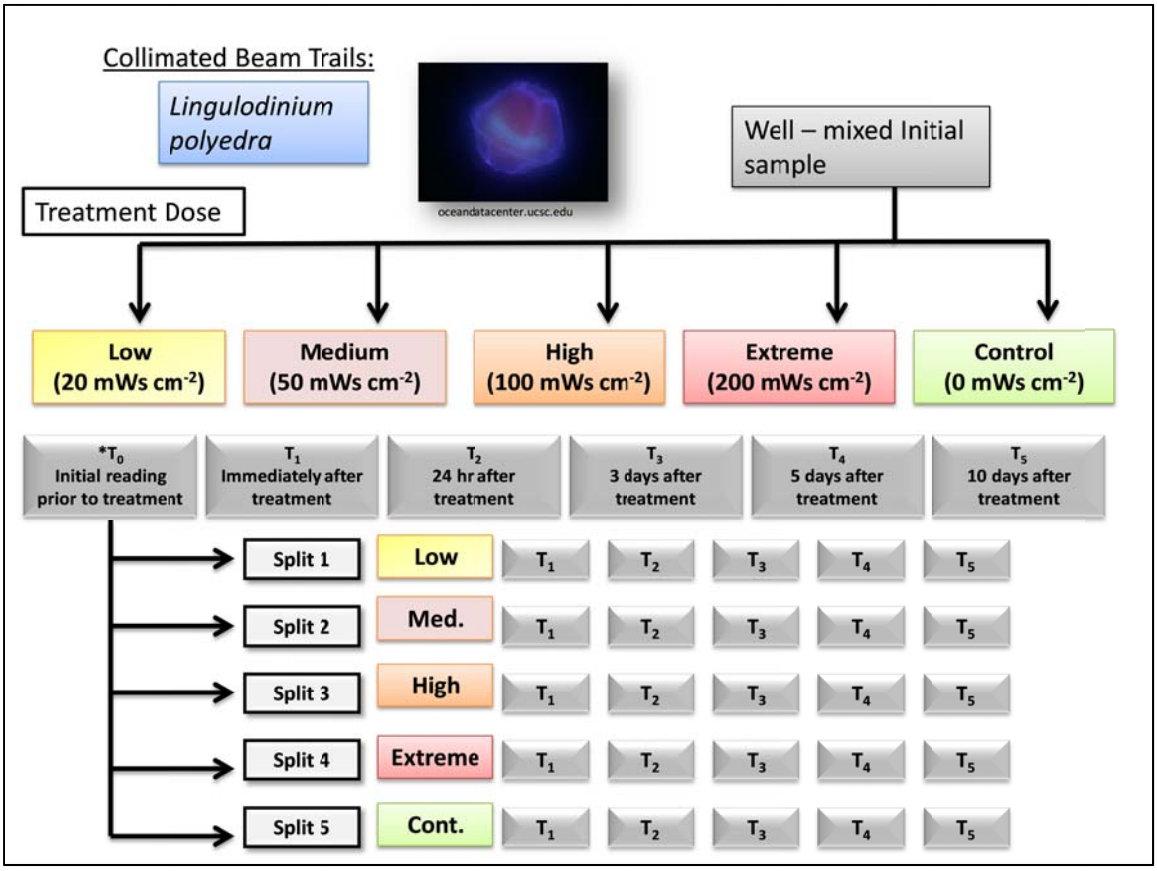

Figure 6: Overview of the experimental approach for the UV Collimated Beam. * Initial readings were used to verify target concentrations (1000 – 3000 mL^{-1}) and to check the physiological status (via PAM fluorometry) of organisms prior to treatment. This data is not shown.

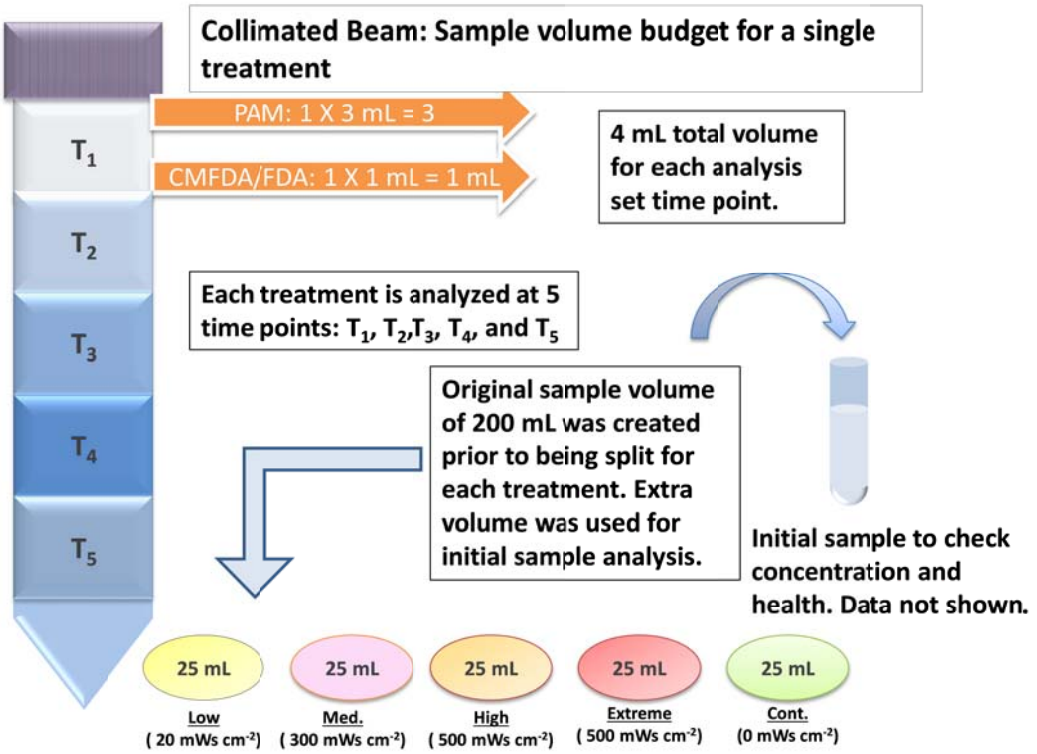

Figure 7: Sample volume ration for a single treatment during the UV collimated beam trials.

6. Manual Epifluorescence Microscopy

6.1. Fluorescent Labeling of *Lingulodinium polyedra*

Samples of *L. polyedra* were labeled with a combination of viability stains; fluorescein diacetate (FDA, 5 µM) and chloromethylfluorescein diacetate (CMFDA, 2.5 µM final concentration). Fluorescein diacetate is a non-fluorescent molecule that can pass freely through cell membranes. Within cells, non-specific esterases cleave to the acetate groups from the molecule to create the product fluorescein, which is both fluorescent under blue light excitation and considerably membrane-impermeable, thus is retained within living cells with intact membranes. The second stain, CMFDA, has similar characteristics, but its methyl group is slightly thiol-reactive, so the molecule binds to the thiol groups within the cell and leads to better cellular retention than FDA. However, the fluorescent signal of CMFDA is not as intense as FDA, which is why both stains are required (Steinberg et al. 2011).

This method is described in detail elsewhere (Steinberg et al. 2011). Briefly, FDA and CMFDA were directly added to a sample of *L. polyedra* in a 1.5 mL micro-centrifuge tube. The micro-centrifuge tube was incubated in the dark at room

temperature for 30 min. Labeled samples of *L. polyedra* were analyzed within 30 min from the start of the incubation.

6.2. Preparing the Sedgewick Rafter counting slide

Upon completion of the incubation, the 1 mL labeled sample of *L. polyedra* was dispensed into the chamber of a gridded Sedgewick Rafter (SR) counting slide. The size of the SR slide is 50 x 20 x 1 mm (after the cover glass is placed upon the chamber) and contains exactly 1 mL of sample. The bottom surface of the SR slide chamber is gridded with 1000 squares, each 1 x 1 mm. Because the depth of the water column is exactly 1 mm, the sample volume can be determined based upon the area counted; 1 x 1mm square contains 1 µL of sample.

6.3. Counting *L. polyedra*

Labeled samples of *L. polyedra* were counted by examining the SR counting slide (containing 1 mL of sample) on an epifluorescence microscope at 100x magnification (Nikon AZ100, Nikon U.S.A., Melville, NY). The microscope was equipped with both brightfield and epifluorescence illumination. The microscope also had an 8:1 variable zoom used to further assess cells and cysts. Both FDA and CMFDA have similar excitation and emission wavelength parameters, and a standard green fluorescence light filter set was used to detect FDA and CMFDA fluorescence (excitation: 465-496 nm; dichroic mirror: 505, emission 515 – 555).

For each analyzed sample, 7 rows of the SR counting slide were randomly selected and counted (each row is 50 µL) (See Appendix D). *L. polyedra* cells and cyst were first detected in brightfield illumination. Once a *L. polyedra* cell(s) was identified, the brightfield was blocked and the epifluorescence illumination was used to detect the FDA/CMFDA in *L. polyedra* cell(s). If the organism displayed green fluorescence, the *L. polyedra* cell was classified as living (e.g. active). If the cell was non-fluorescing, then the *L. polyedra* cell was classified as dead (e.g. inactive). Cysts were identified during the initial scan using the brightfield illumination and were classified according to morphological criteria (e.g. formation of cyst wall; theca has been shed). Collected data was recorded on data sheets for each sample type (See Appendix C). Cells of *L. polyedra* in brightfield and epifluorescence illumination and a *L. polyedra* cyst in brightfield illumination are displayed in Figure 8. The final concentration of live, dead, and cysts of *L. polyedra* (P = individuals mL^{-1}) were calculated using the following equation,

$$P = \frac{I}{AS}$$

where I is the sum of individual organisms/cysts, A is the volume of sample analyzed, and S is the total sample volume. Manual epifluorescence microscopy was performed at each set time period and significant differences among treatments were identified using a

one-way ANOVA test (UV crosslinker trials: n=3, α = 0.05; UV collimated beam trials: n=5, a=0.05).

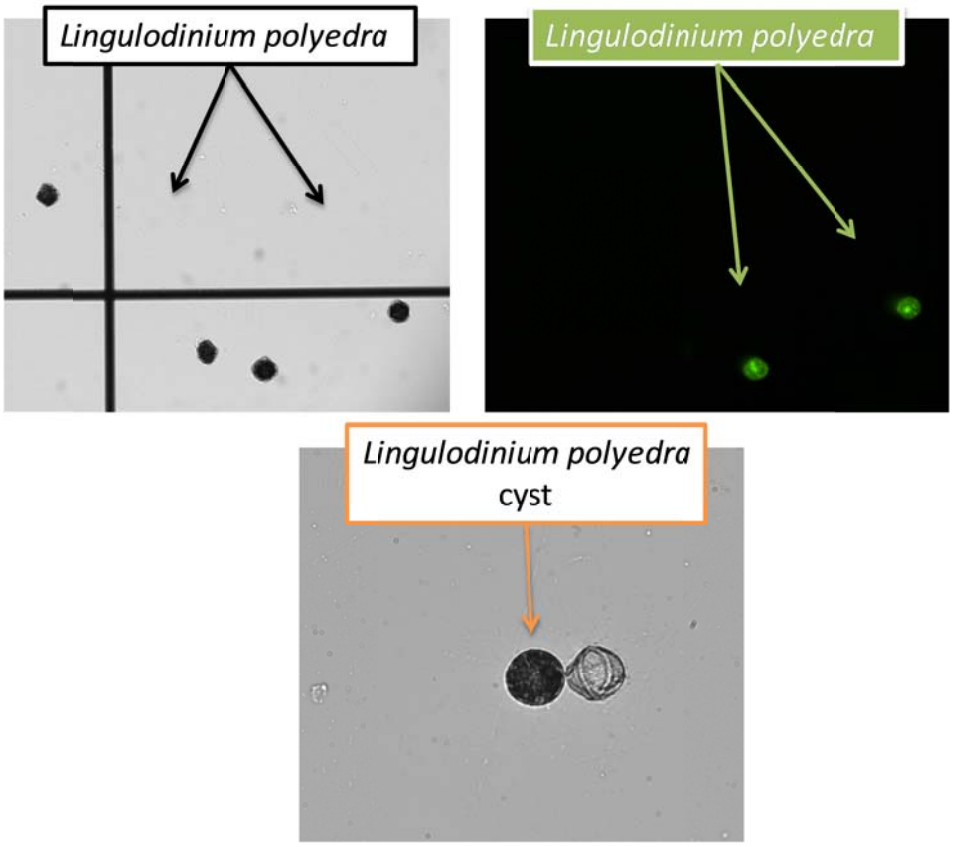

Figure 8: FDA/CMFDA labeled cells of *L. polyedra*. Top left: view of *L. polyedra* in brightfield illumination; top right: view of *L. polyedra* in epifluorescence illumination with FDA/CMFDA detected (e.g. living); and center: view of a *L. polyedra* cyst in brightfield illumination (formation of cyst wall; theca has been shed)

7. Pulse Amplitude Modulated (PAM) Fluorometry

Pulse Amplitude Modulated (PAM) fluorometry is rapid analytical approach, which estimates chlorophyll a fluorescence (F_0) and the physiological state (Y) of photosynthetic organisms (Genty et al 1989). The photochemical yield (Y), is a relative measure of electron transport efficiency and is calculated by the initial (F_0) and maximum saturated (F_m) chlorophyll a fluorescence's at saturating light intensities (Y; $(F_m - F_0)/F_m$). The Y values generally reflect the rates of algal production (Barranguet C. and Kromkamp J. 2000) which, then corresponds to a living and actively productive algal community. In contrast, low Y values suggest chlorophyll a fluorescence originating from dead or biological aging organisms (First R. M. and L. A. Drake, 2013).

PAM fluorometry was performed using the WaterPAM™ fluorometer: WATER-ED Emitter –Detector with PAM-CONTROL Universal Control Unit and the automated

WinControl software (Walz, GmbH, Effeltrich, Germany). Individual well-mixed samples of *Lingulodinium polyedra* (3 mL) were dispensed into a quartz cuvette and then placed in the WATER-ED Emitter –Detector. After 10 sec to allow the initial fluorescence (F_0) to stabilize, the analysis was started using the WinControl automated software. Three measurements of the initial fluorescence (F_0), maximum fluorescence (F_m), and photochemical yield (Y) were collected every 10 sec for each analytical replicate sample. The data collected from the WinControl software was extracted using a MATLAB routine and used to generate final results. PAM fluorometry was performed at set time periods and significant differences among treatments were identified using a one-way ANOVA (UV crosslinker trials: n=3, $\alpha = 0.05$; UV collimated beam trials: n=5, a=0.05).

V. Results

1. UV Crosslinker Trials

Three trials were performed to compare the viability signal and organism response of *Lingulodinium polyedra* following UV treatment at multiple UV doses: low UV (100 mWs cm^{-2}), medium UV (300 mWs cm^{-2}), high UV (500 mWs cm^{-2}), and control (0 mWs cm^{-2}). The experiments using the crosslinker account for the high end treatments. The concentration of live, dead, and *L. polyedra* cysts as well PAM fluorometry results are described in the following sections.

1.1. Live *L. polyedra* - Manual epifluorescence microscopy

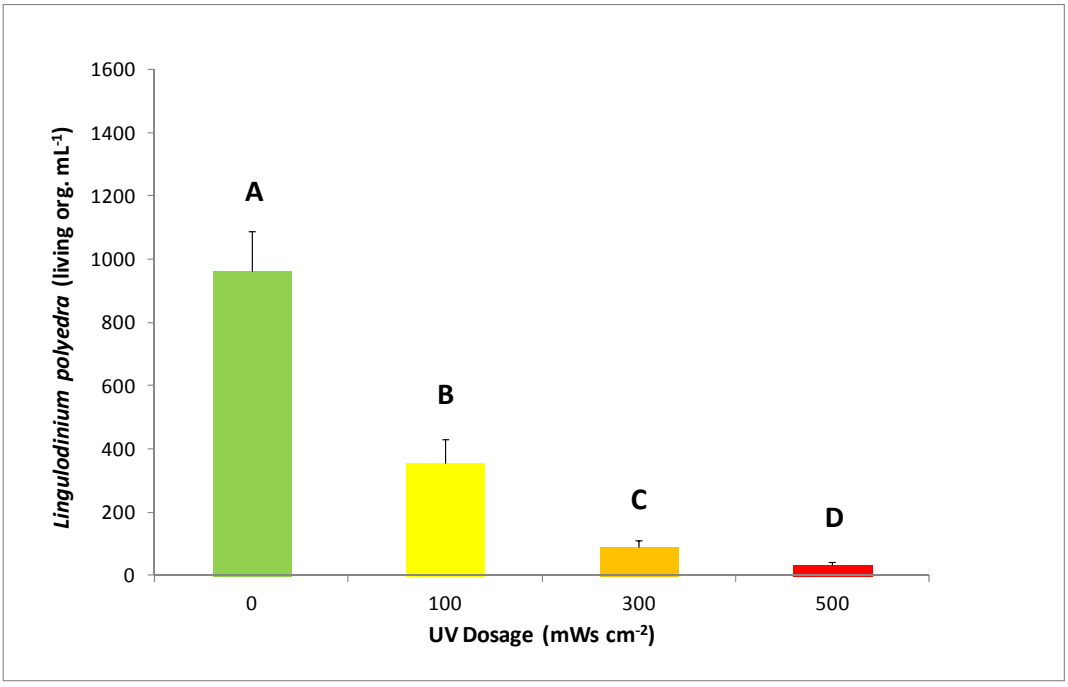

Figure 9: Concentration of Living *L. polyedra* (living org. mL^{-1}) determined by epifluorescence microscopy for each UV treatment using the UV crosslinker. The letters represent significant differences and the bars show the mean concentration (± 1 SD) of 3 replicates over three set analysis time periods (Day 0, Day 1,and Day 3) (ANOVA, $p > 0.05$).

All treated samples of *L. polyedra* were significantly less than the control (961 ± 128 living org. mL^{-1}) as shown in Figure 9. Due to the significant difference in living concentrations of *L. polyedra* between the control and the UV treated samples, the null hypothesis is rejected.

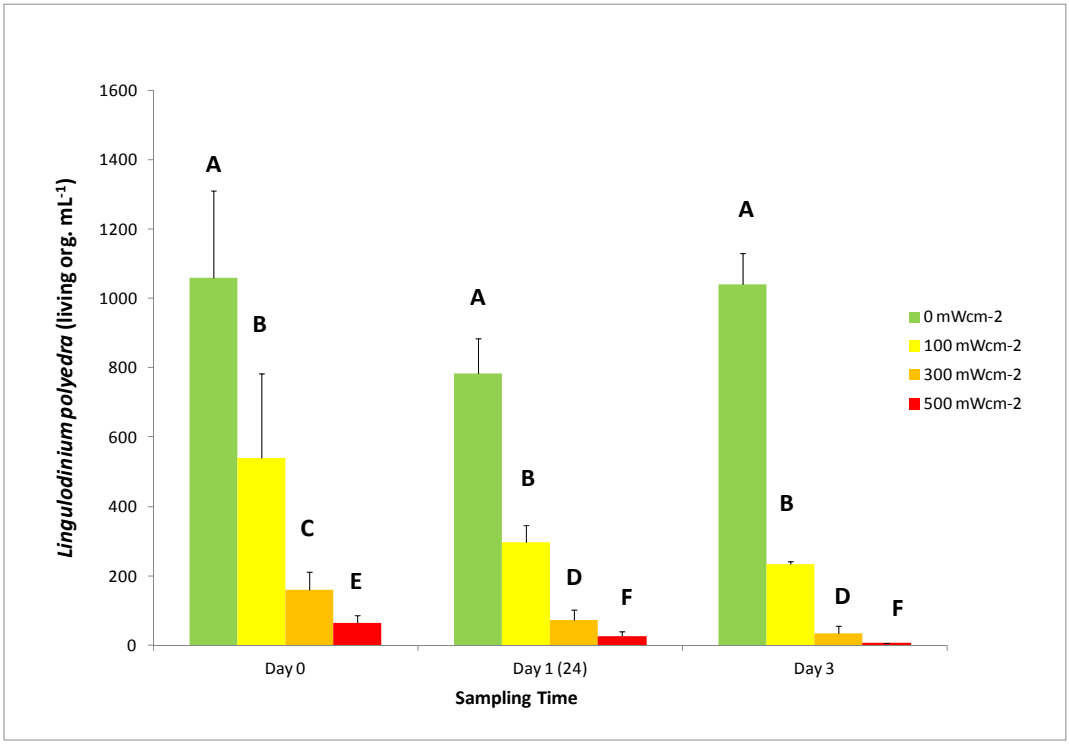

Figure 10: Concentration of living *L. polyedra* (living org. mL^{-1}) at different UV treatments using the crosslinker over the epifluorescence microscopy sample analysis time. The bars show the mean concentration (± 1 SD) of 3 replicates for each treatment over time. The letters represent significant differences among sample (ANOVA, $p > 0.05$).

There is no significant difference in living concentration of *L. polyedra* in the control sample over the manual epifluorescence microscopy sample analysis time period (ANOVA, $p = 0.154$) as presented in Figure 10. This is also true for the samples treated at 100 mWs cm^{-2} (ANOVA, $p = 0.86$). The living concentration of *L. polyedra* decreased from Day 0 (161 ± 51 living org. mL^{-1}) to Day 1 (73 ± 31 living org. mL^{-1}) and were significantly different when treated at 300 mWs cm^{-2}, but the concentration did not

significantly decrease from Day 1 to Day 3 (34 ± 21 living org. mL^{-1}) (ANOVA, p= 0.235). The results for samples treated at 500 mWs cm^{-2} were similar, as there was a significant decrease in living *L. polyedra* concentrations from Day 0 (64 ± 22 living org. mL^{-1}) to Day 1 (26 ± 15 living org. mL^{-1}), but no significant decrease from Day 1 to Day 3 (6 mL^{-1} ± 2 living org. mL^{-1}) (ANOVA, p= 0.169).

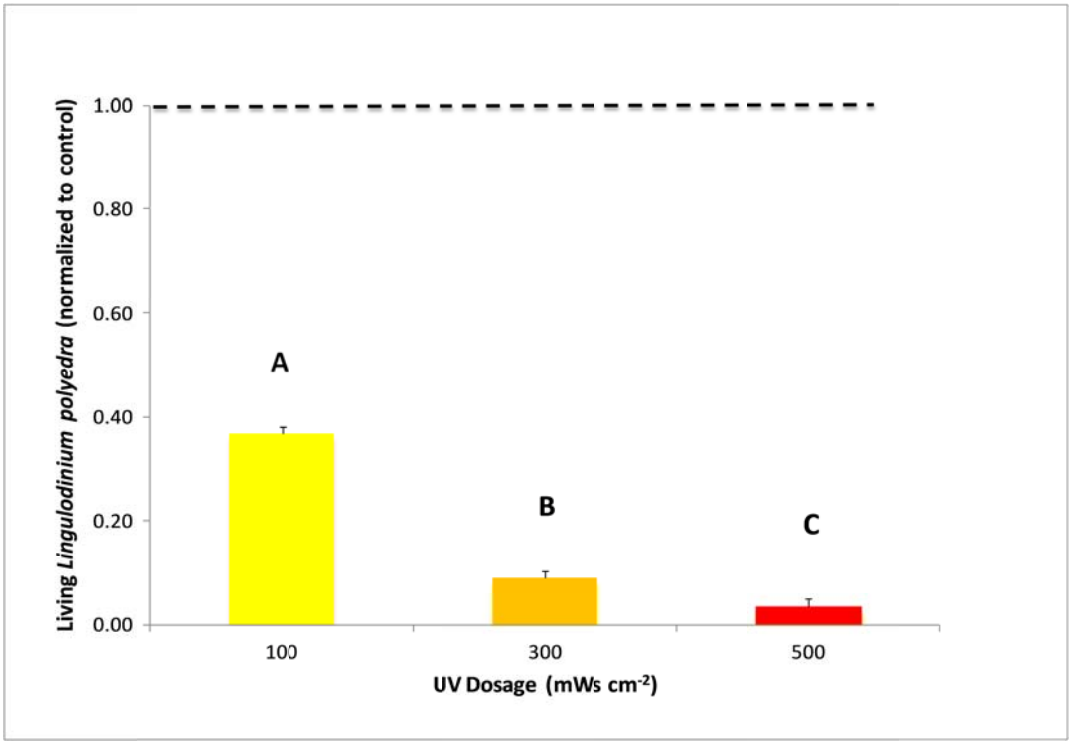

Figure 11: Normalized living concentrations of *L. polyedra* of each UV treatment using the UV crosslinker. The bars show the normalized mean of the three epifluorescence microscopy analytical replicates (Day 0, Day 1, and Day 3) and the dotted line marks equal concentration to the control. The letters represent significant differences (ANOVA, $p > 0.05$).

Shown in Figure 11 are treated samples of living *L. polyedra* normalized to the control (normalized = treated/control). Each normalized treated sample of living concentrations of *L. polyedra* were significantly different (ANOVA, $p > 0.05$). The live concentration of *L. polyedra* in the samples treated at 100 mWs cm^{-2} roughly correlates to 37 % of the control (decrease of 63%). The samples treated at 300 mWs cm^{-2} decreased by roughly 91 % (9% ± 1%) to the control and the samples treated at 500 mWs cm^{-2} decreased by nearly 97% (3% ± 2%) to the control. These results reject the null hypothesis as the increase in UV treatment decreases the viability signal when measuring viability by manual epifluorescence microscopy.

1.2. Dead *L. polyedra* - Manual epifluorescence Microscopy

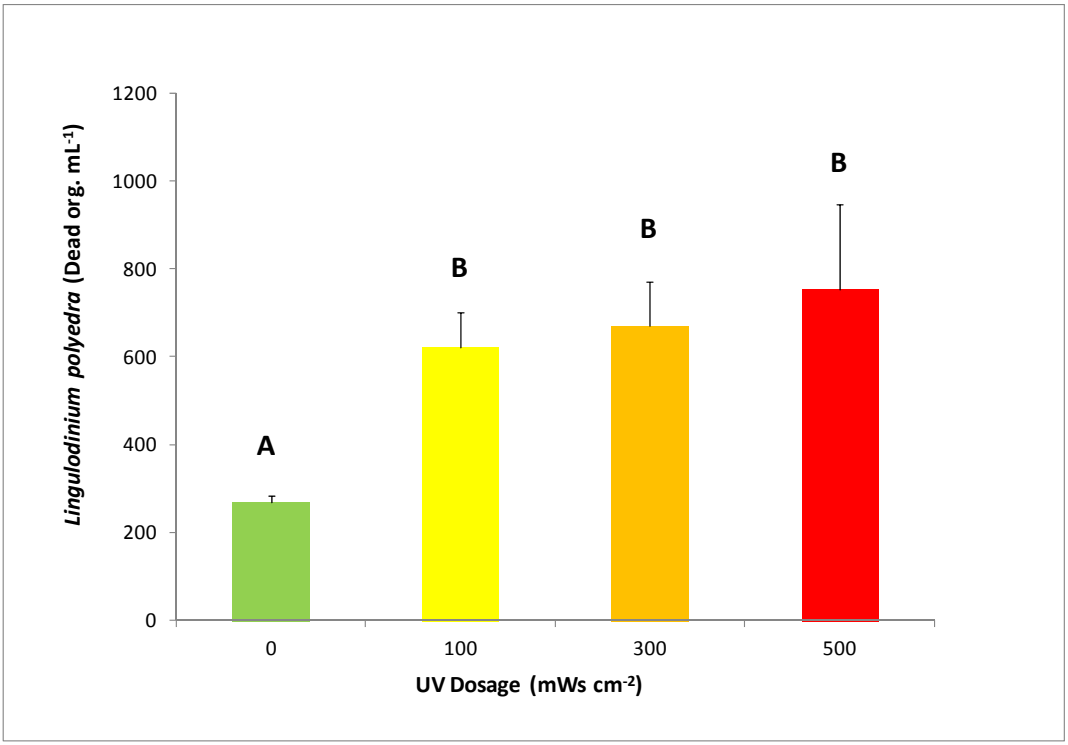

Figure 12: Concentration of dead *L. polyedra* (dead org. mL^{-1}) determined by epifluorescence microscopy for each UV treatment using the UV crosslinker. The letters represent significant differences and the bars show the mean concentration (± 1 SD) of 3 replicates over three set analysis time periods (Day 0, Day 1, and Day 3) (ANOVA, $p > 0.05$).

Shown in Figure 12, the concentration of dead *L. polyedra* in the control sample (267 ± 16 dead org. mL^{-1}) is significantly less than each of the treated samples (ANOVA, $p > 0.05$). Regarding the UV treated samples (100, 300, and 500 mWs cm^{-2}) there is no significant difference in the concentration of dead *L. polyedra* between each treatment. The increase in dead concentration of *L. polyedra* of treated samples correlates to the decrease in live concentrations treated by UV radiation as seen in Figure 9.

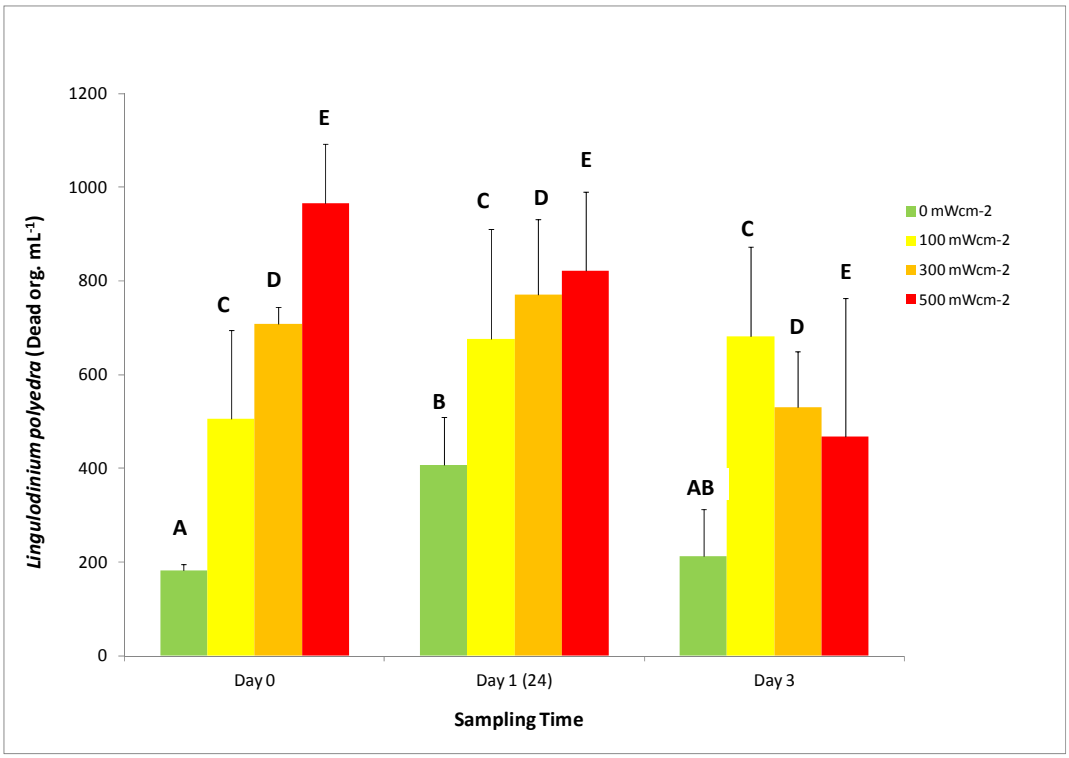

Figure 13: Concentration of dead *L. polyedra* (dead org. mL^{-1}) at different UV treatments using the crosslinker over the epifluorescence microscopy sample analysis time. The bars show the mean concentration (± 1 SD) of 3 replicates for each treatment over time. The letters represent significant differences (ANOVA, $p > 0.05$).

As displayed in Figure 13, there was a significant increase in the concentration of dead *L. polyedra* from Day 0 (182 ± 13 dead org. mL^{-1}) to Day 1 (407 ± 103 dead org. mL^{-1}) in the control sample, but the dead concentration of *L. polyedra* decreased by Day 3 (212 ± 100 dead org. mL^{-1}), as there was no significant difference between Day 0 and Day 3. Viewing the treated samples in Figure 13, there was no significance difference over the sample analysis time period (Day 0, Day 1, and Day 3) of dead *L. polyedra* concentration in samples treated at 100 mWs cm^{-2} (ANOVA, p= 0.528), 300 mWs cm^{-2} (ANOVA, p= 0.100), and the 500 mWs cm^{-2} (ANOVA, p= 0.064).

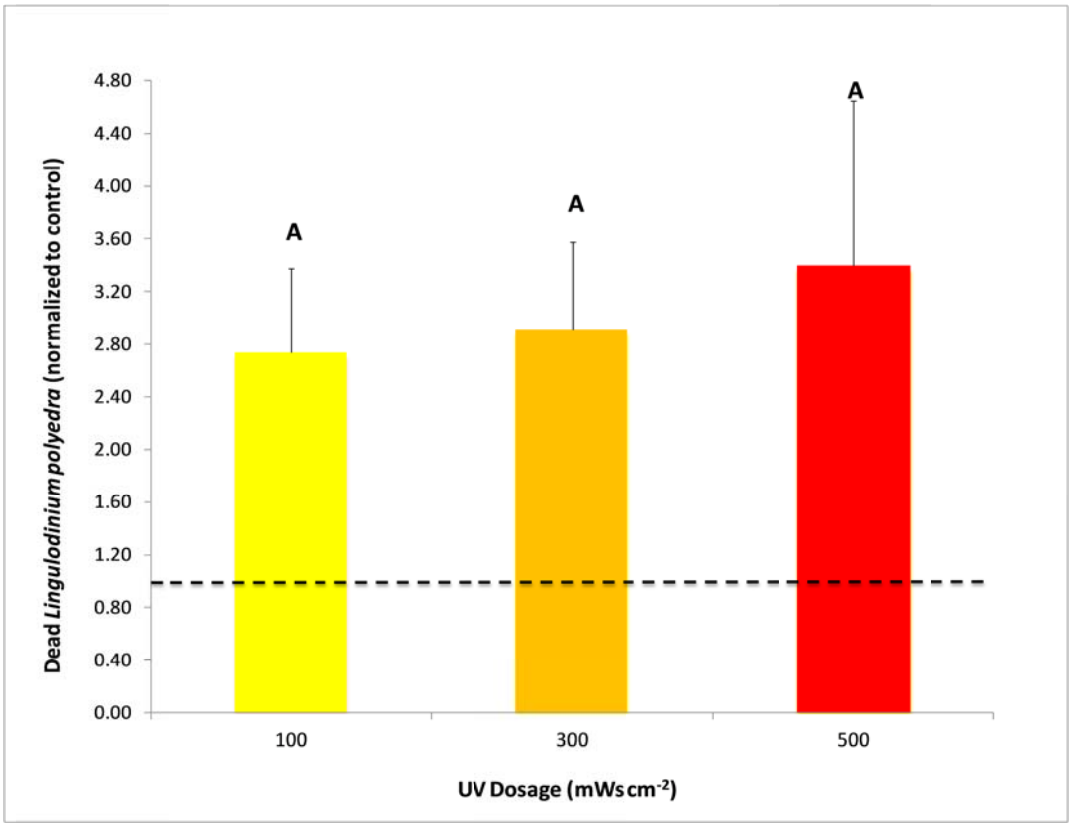

Figure 14: Normalized dead concentrations of *L. polyedra* of each UV treatment using the UV crosslinker. The bars show normalized mean of the three epifluorescence microscopy analytical replicates (Day 0, Day 1, and Day 3) and the dotted line marks equal concentration to the control. The letters represent significant differences (ANOVA, $p > 0.05$).

The dead concentrations of *L. polyedra* that are normalized to the control (normalized = treated/control) are displayed in Figure 14. Because the concentrations of dead *L. polyedra* were higher than in the control sample, the values are above the dotted line, which marks equal concentration to the control (1.00). There was no significant difference between the normalized treated samples of the dead concentration of *L. polyedra* (ANOVA, $p= 0.660$). Dead organisms were roughly 2 fold more concentrated than living cells, indicating the efficacy of UV treatment.

1.3. *L. polyedra* cysts - Manual epifluorescence microscopy

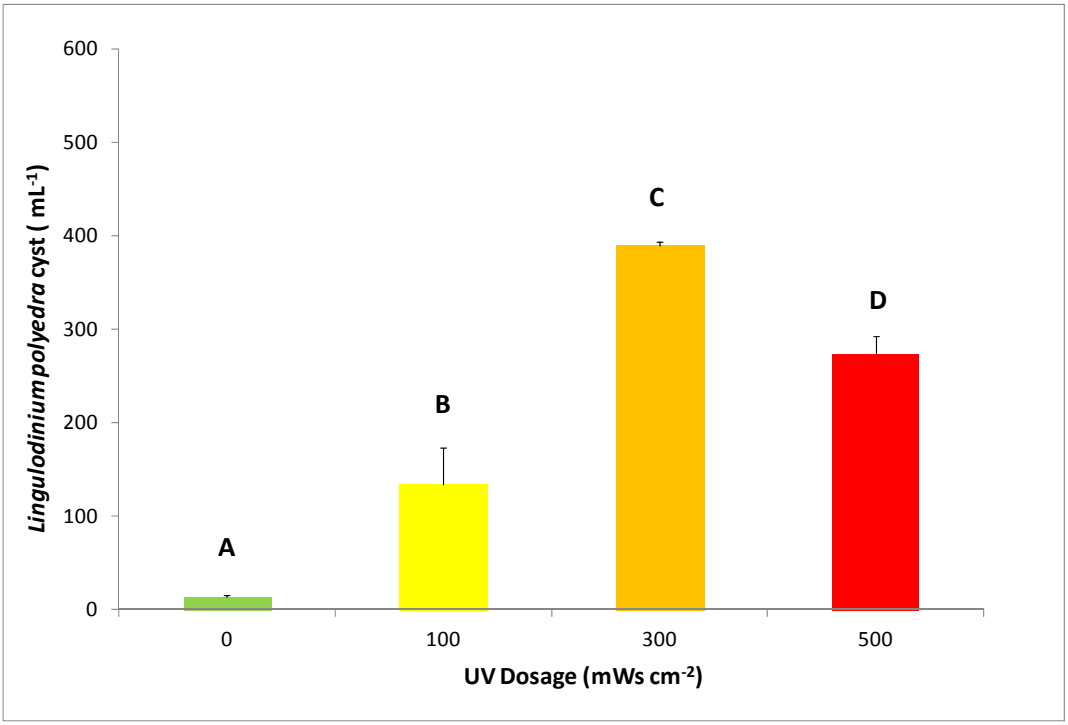

Figure 15: Concentration *L. polyedra* cysts (cysts mL^{-1}) determined by epifluorescence microscopy for each UV treatment using the UV crosslinker. The letters represent significant differences and the bars show the mean concentration (± 1 SD) of 3 replicates over three set analysis time periods (Day 0, Day 1, and Day 3) (ANOVA, $p > 0.05$).

Each analyzed sample of *L. polyedra* had a significantly different concentration of *L. polyedra* cysts (ANOVA, $p > 0.05$) and the treated samples were significantly higher than the control (Figure 15). The samples treated at 300 mWs cm^{-2} had the highest concentration of cysts at 389 (± 4) cysts mL^{-1} followed by the samples treated at 500 mWs cm^{-2} with 274 (± 19) cysts mL^{-1} and then 100 mWs cm^{-2} having a concentration 134 (± 40) *L. polyedra* cysts mL^{-1}. The control samples had a *L. polyedra* cyst concentration of 14 (± 1) cysts mL^{-1}.

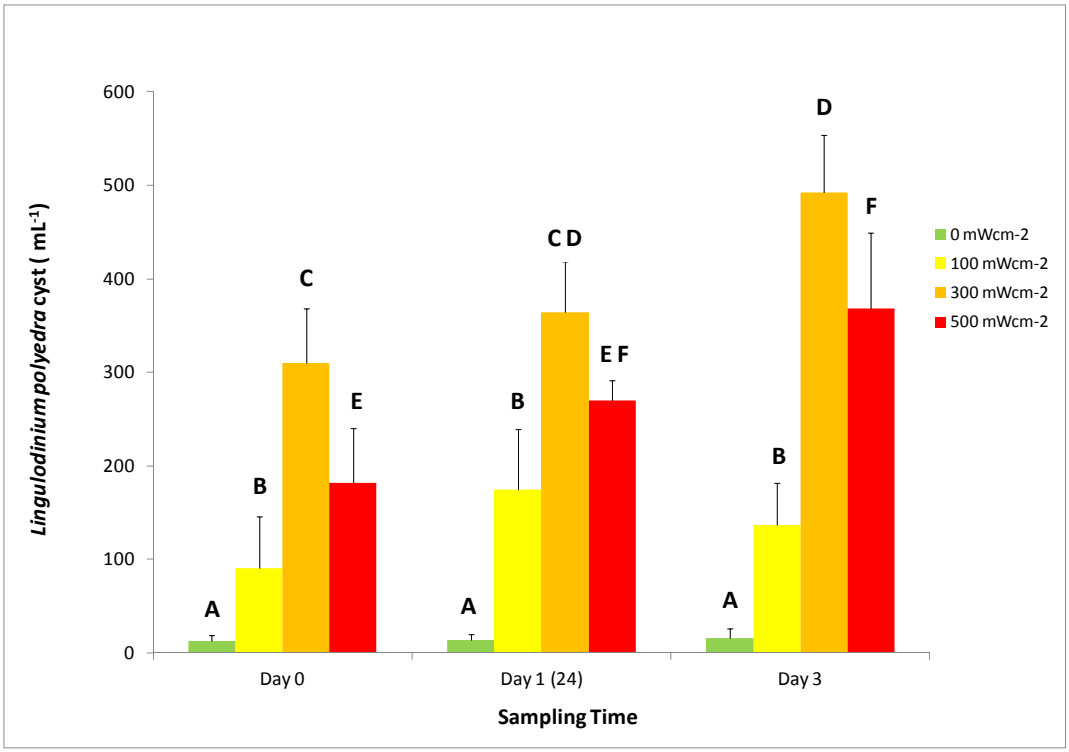

Figure 16: Concentration of *L. polyedra* cysts (cysts mL-1) at different UV treatments using the crosslinker over the epifluorescence microscopy sample analysis time. The bars show the mean concentration (± 1 SD) of 3 replicates for each treatment over time. The letters represent significant differences (ANOVA, $p > 0.05$).

Shown Figure 16, the concentration of *L. polyedra* cysts in the control samples did not increase or decrease during the sample analysis time period (ANOVA, $p = 0.901$). The concentration of *L. polyedra* cysts in the samples treated at 100 mWs cm^{-2} also did not change significantly over the manual epifluorescence microscopy sample analysis time period (ANOVA, $p= 0.254$). Viewing the cyst concentrations in the samples treated at 300 mWs cm^{-2}, the concentration did not significantly increase from Day 0 (310 ± 58 cysts mL^{-1}) to Day 1 (364 ± 54 cysts mL^{-1}), but the cyst concentration were significantly different from Day 0 to Day 3 (493 ± 62 cysts mL^{-1}). The results for the *L. polyedra* samples treated at 500 mWs cm^{-2} were similar to those at treated at 300 mWs cm^{-2}, as there was no significant difference in cyst concentration from Day 0 (182 ± 59 cysts mL^{-1}) to Day 1 (270 ± 21 cysts mL^{-1}), but a significant difference in cyst concentration from Day 0 to Day 3 (369 ± 81 cysts mL^{-1}). For samples treated at 300 and 500 mWs cm^{-2}, the concentration of *L. polyedra* cysts increased over the sample analysis time period.

1.4. PAM Fluorometry - Photochemical Yield (*Y*)

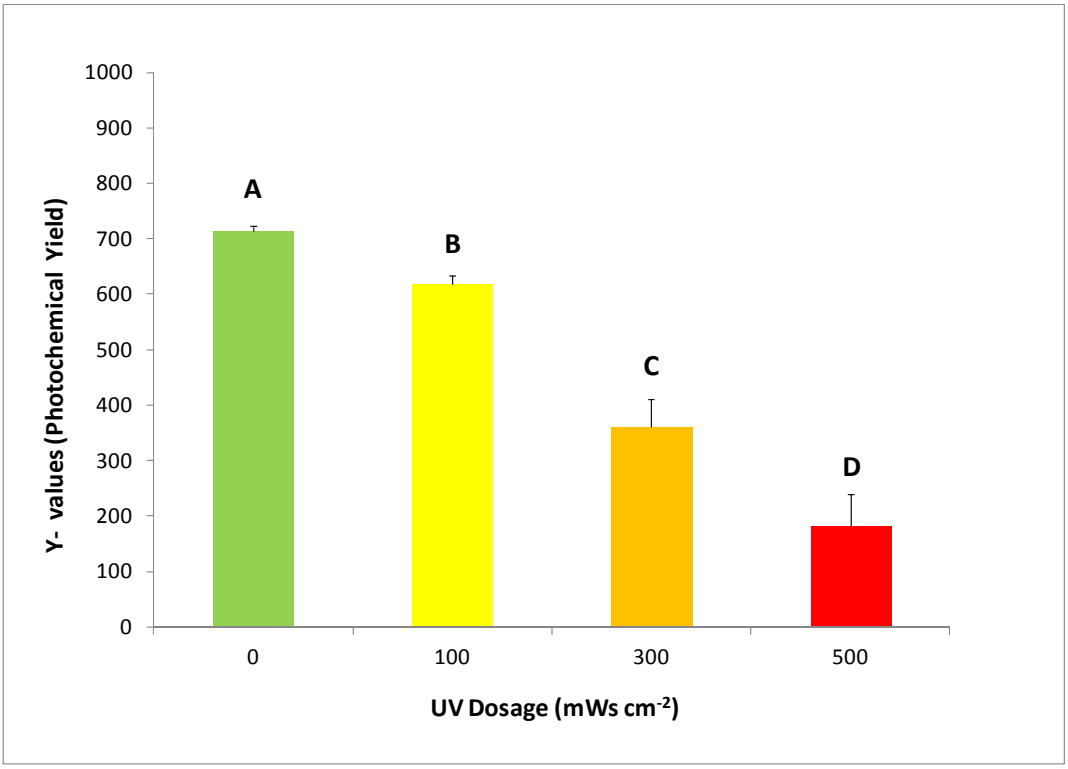

Figure 17: The photochemical yield (Y) of *L. polyedra* determined by PAM fluorometry for each UV treatment using the UV crosslinker. The letters represent significant differences and the bars show the mean concentration (± 1 SD) of 3 replicates over three set analysis time periods (Day 0, Day 1, and Day 3).

The photochemical yield (*Y*) results of each analyzed *L. polyedra* sample are presented in Figure 17. Each measured sample of *L. polyedra* is significantly different and there is a significant decline in the photochemical yield from the control to the treated samples (ANOVA, $p > 0.05$). Observing the viability signal of *L. polyedra* measured by PAM fluorometry, the null hypothesis is rejected as the photochemical yield significantly decreases with the increase in UV radiation.

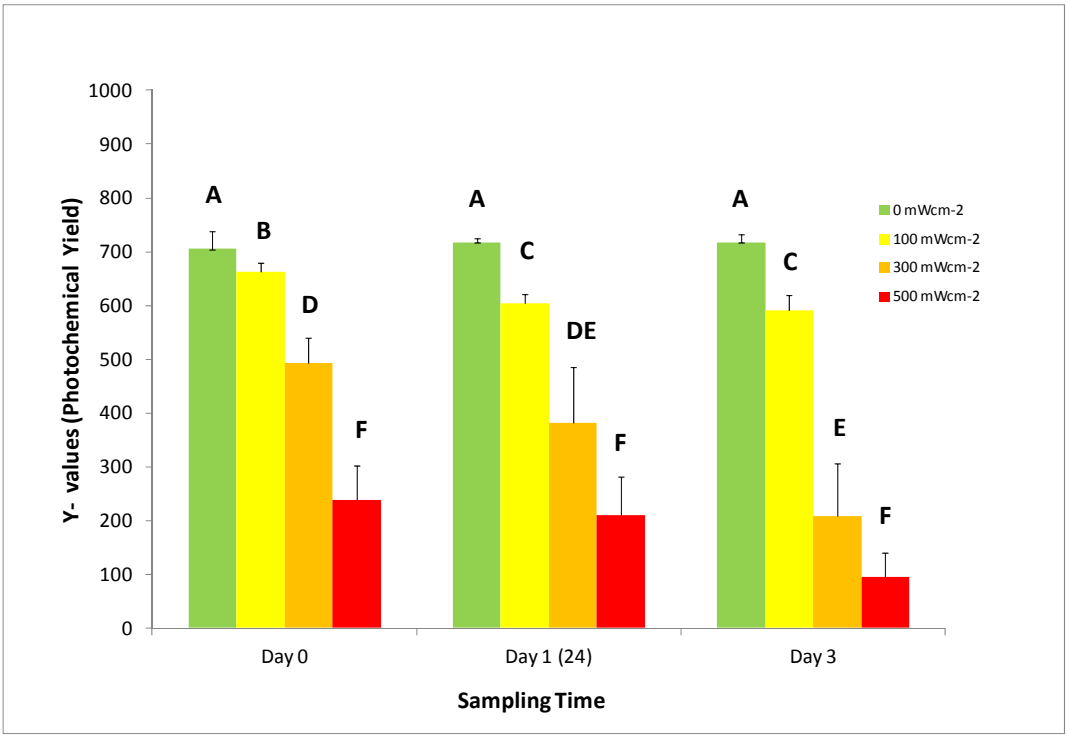

Figure 18: The photochemical yield (*Y*) of *L. polyedra* samples determined by PAM fluorometry over the sample analysis time. The bars show the mean concentration (± 1 SD) of 3 replicates for each treatment over time. The letters represent significant differences (ANOVA, $p > 0.05$).

There was no significant difference in the photochemical yield of the control samples over the 3 analysis time periods (ANOVA, $p = 0.727$) (Figure 18). Viewing the samples treated at 100 mWs cm^{-2}, there was a significant decline in photochemical yield from Day 0 (662 ± 17 *Y* value) to Day 1 (603 ± 18 *Y* value), but no further significant decline from Day 1 to Day 3 (590 ± 28 *Y* value). Observing the *L. polyedra* samples treated at 300 mWs cm^{-2}, there was no significant difference from Day 0 (492 ± 47 *Y* value) to Day 1 (382 ± 104) in measured photochemical yield, but there was a significant decline from Day 1 to Day 3 (209 ± 99). There was no significant change in measured photochemical yield of *L. polyedra* samples treated at 500 mWs cm^{-2} (ANOVA, $p = 0.065$), as all measure samples were below a *Y* value of 300 over the entire analysis time period.

2. UV Collimated Beam Trials

Three trials were conducted to compare the viability signal and organism response of *Lingulodinium polyedra* following UV treatment at different doses using the UV collimated beam; low UV (20 mWs cm^{-2}), medium UV (50 mWs cm^{-2}), high UV (100 mWs cm^{-2}), extreme UV (200 mWs cm^{-2}), and control (0 mWs cm^{-2}). The experiments using the collimated beam account for the low end UV treatments. The analysis time period was also extended to examine the response over a longer period of time. The concentration of live, dead, and *L. polyedra* cysts and PAM fluorometry are present in the following sections.

2.1. Live *L. polyedra* – Manual epifluorescence Microscopy

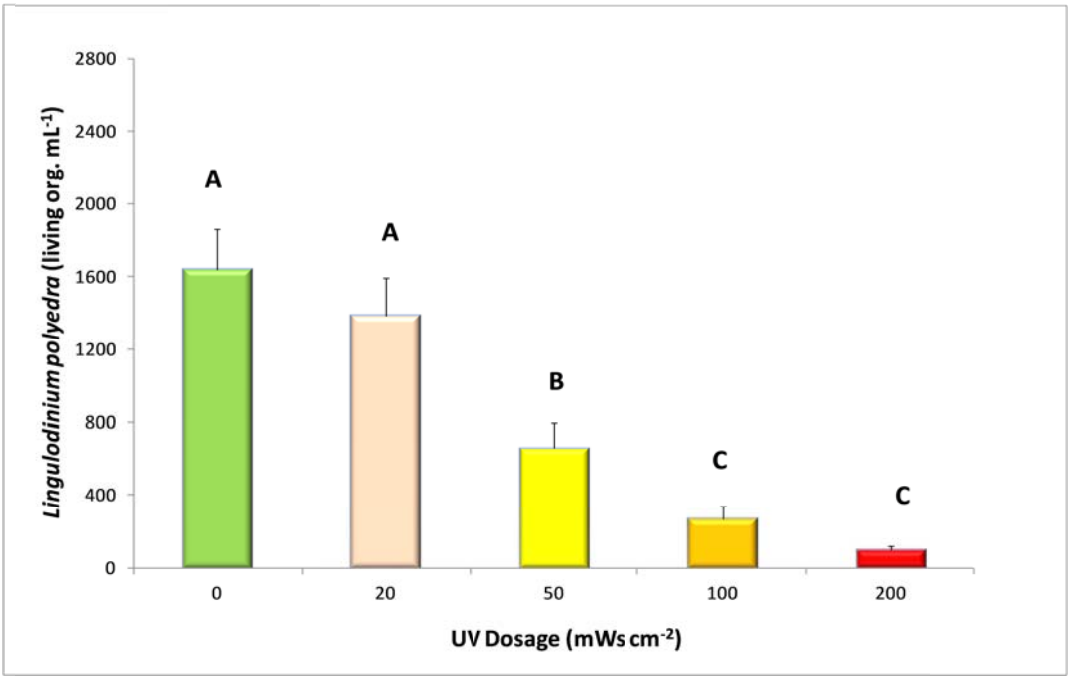

Figure 19: Concentration of Living *L. polyedra* (living org. mL^{-1}) determined by epifluorescence microscopy for each UV treatment using the UV collimated beam. The letters represent significant differences and the bars show the mean concentration (± 1 SD) of 3 replicates over three 5 analysis time periods (Day 0, Day 1, Day 3, Day 5, and Day 10) (ANOVA, $p > 0.05$).

Figure 19 shows no significant difference in living concentration between the control and the sample treated at 20 mWs cm^{-2} (ANOVA, $p = 0.065$). There was a significant decline in the living concentration of *L. polyedra* at 50, 100, and 200 mWs cm^{-2} relative to the control.

For treatments above 50 mWs cm^{-2}, the null hypothesis is rejected as the increase in UV treatment decrease the viability signal when samples are measure by manual epifluorescence microscopy. There was no significant difference in living concentrations between samples treated at 100 and 200 mWs cm^{-2} (ANOVA, $p = 0.193$) and the null hypothesis is not rejected at these UV treatment doses, but concentrations were dramatically less than the control for both treated samples (100 mWs cm^{-2}: 270 ± 67 living org. mL^{-1}; 200 mWs cm^{-2}: 98 ± 24 living org. mL^{-1}).

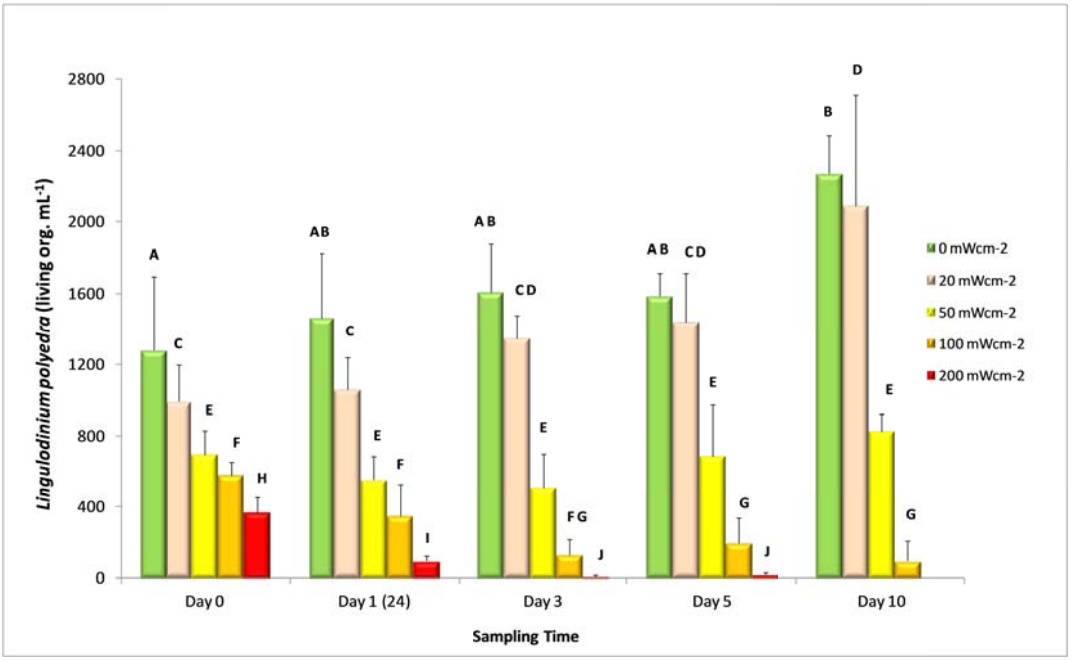

Figure 20: Concentration of living *L. polyedra* (living org. mL-1) at multiple UV treatments using the collimated beam over the epifluorescence microscopy sample analysis time. The bars show the mean concentration (± 1 SD) of 3 replicates for each treatment over time. The letters represent significant differences among sample (ANOVA, $p > 0.05$).

Viewing Figure 20, there was no significant difference in the concentration of living *L. polyedra* in the control samples until Day 10, when there was a significant increase in concentration when comparing Day 0 (1281 ± 418 living org. mL^{-1}) to Day 10 (2267 ±221 living org. mL^{-1}). The results of the samples treated at 20 mWs cm^{-2} were similar to the control as there was a significant increase in concentration from Day 0 (992 ± 205 living org. mL^{-1}) and Day 1 (1059 ± 182 living org. mL^{-1}) and then increasing on Day 10 (2089 ±627 living org. mL^{-1}). There was no significant difference over the analysis time period of the living concentration of *L. polyedra* when treated at 50 mWs cm^{-2} (ANOVA, $p = 0.287$). Viewing the samples treated at 100 mWs cm^{-2}, there was no significant decrease in living concentration until Day 5 The living concentration of *L. polyedra* in the samples treated at 200 mWs cm^{-2} significantly decreased from Day 0 (368

± 86 living org. mL^{-1}) to Day 1 (95 ± 29 living org. mL^{-1}) and the again from Day 1 to Day 3 (9 ± 8 living org. mL^{-1}). There were no identified living concentrations *L. polyedra* treated at 200 mWs cm^{-2} by Day 10 using the manual epifluorescence microscopy method.

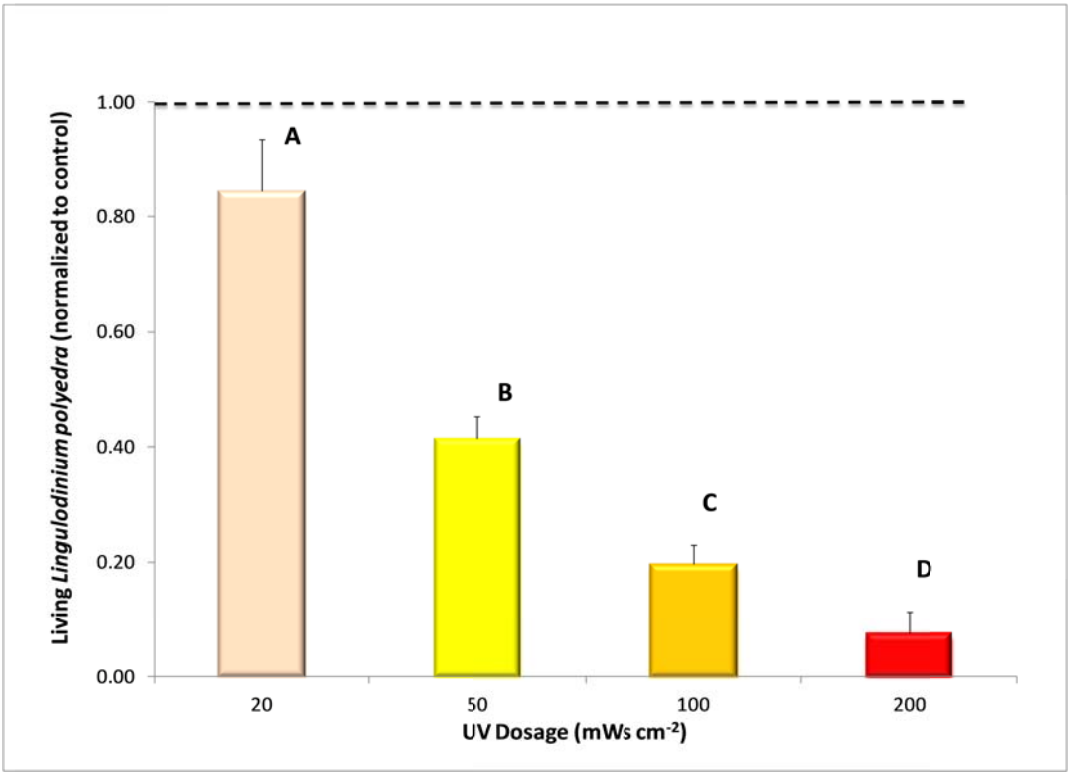

Figure 21: Normalized living concentrations of *L. polyedra* of each UV treatment using the collimated beam. The bars show the normalized mean of the five epifluorescence microscopy analytical replicates (Day 0, Day 1, Day 3, Day 5, and Day 10) and the dotted line marks equal concentration to the control. The letters represent significant differences (ANOVA, $p > 0.05$).

Displayed in Figure 21 are the treated samples of living *L. polyedra* normalized to the control (normalized = treated/control). Each normalized treated sample was significantly different in living concentrations of *L. polyedra* (ANOVA, $p > 0.05$). These results also reject the null hypothesis as the increase in UV treatment decreases the viability signal when viability is measured by manual epifluorescence microscopy.

2.2. Dead *L. polyedra* - Manual epifluorescence Microscopy

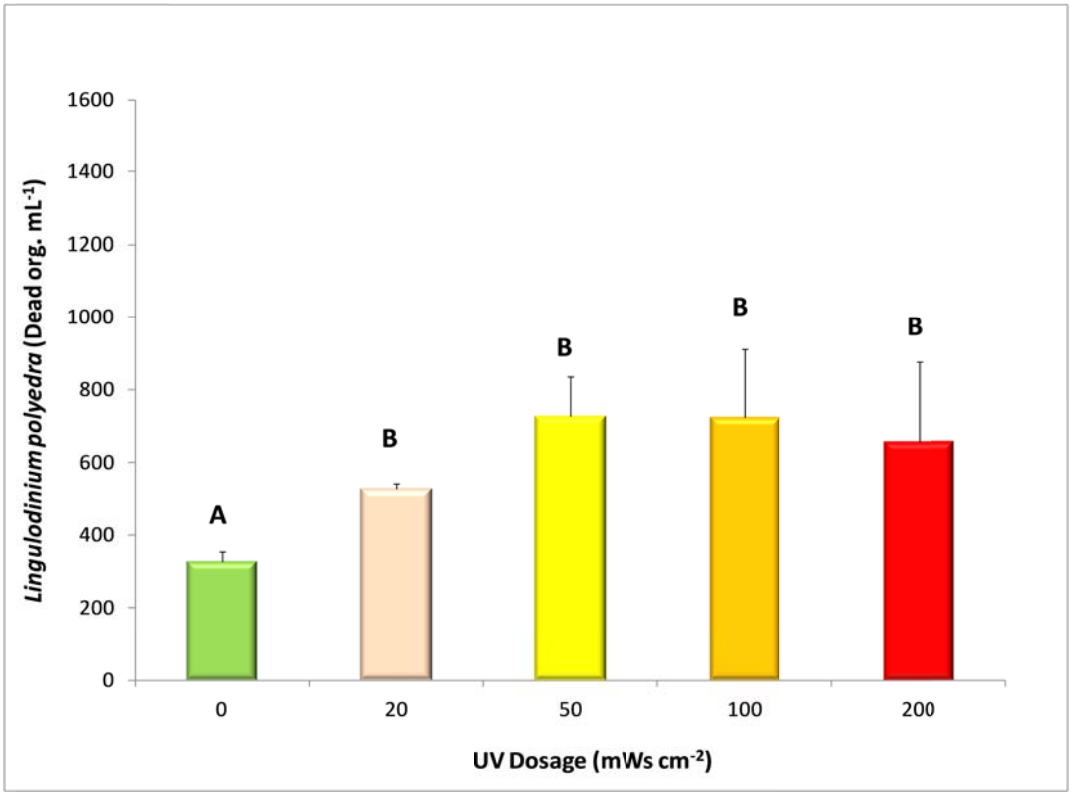

Figure 22: Concentration of dead *L. polyedra* (dead org. mL^{-1}) determined by epifluorescence microscopy for each UV treatment using the UV collimated beam. The letters represent significant differences and the bars show the mean concentration (± 1 SD) of 3 replicates over five set analysis set time periods (Day 0, Day 1, Day 3, Day 5, and Day 10)(ANOVA, $p > 0.05$).

The dead concentration of *L. polyedra* in control sample (329 ± 26 dead org. mL^{-1}) was significantly less than the four treated samples (ANOVA, $p > 0.05$) (Figure 22). There was no significant difference in dead concentration of *L. polyedra* between each of the treated samples (20, 50, 100, and 200 mWs cm^{-2}). This increase in dead concentrations relatively correlates to the living concentrations of *L. polyedra* when viability is determined by manual epifluorescence microscopy (Figure 19).

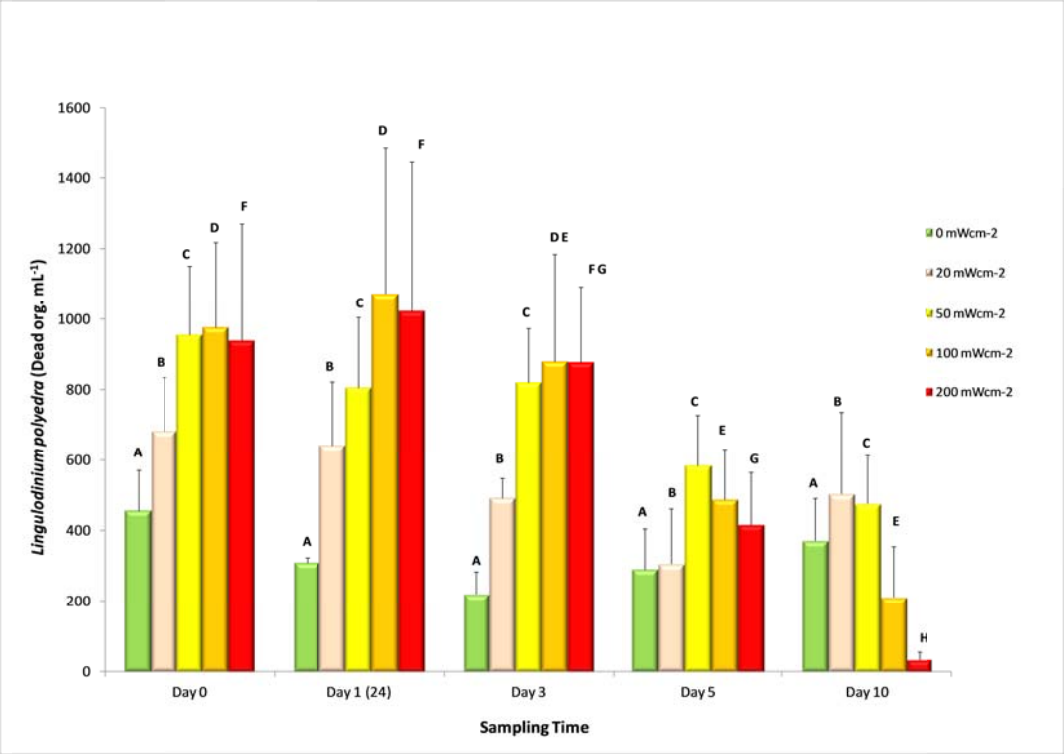

Figure 23: Concentration of dead *L. polyedra* (dead org. mL-1) at multiple UV treatments using the collimated beam over the epifluorescence microscopy sample analysis time period. The bars show the mean concentration (± 1 SD) of 3 replicates for each treatment over time. The letters represent significant differences among sample (ANOVA, $p > 0.05$).

Figure 23 shows there was no significant difference in *L. polyedra* dead concentration in the control sample over the entire sample analysis time period (ANOVA, $p = 0.099$). This was also true for samples treated at 20 mWs cm^{-2} (ANOVA, $p = 0.121$) and samples treated at 50 mWs cm^{-2} (ANOVA, $p = 0.058$). Viewing the dead concentrations of *L. polyedra* treated at 100 mWs cm^{-2}, there was a significant decrease from Day 3 (820 ± 154 dead org. mL^{-1}) to Day 5 (585 ± 142 dead org. mL^{-1}) and Day 10 (476 ± 138). The samples treated at 200 mWs cm^{-2} significantly decrease in dead concentration at Day 3 (877 ± 215 dead org. mL^{-1}) to Day 5 (416 ± 149 dead org. mL^{-1}) and then again at Day 10 (32 ± 23 dead org. mL^{-1})

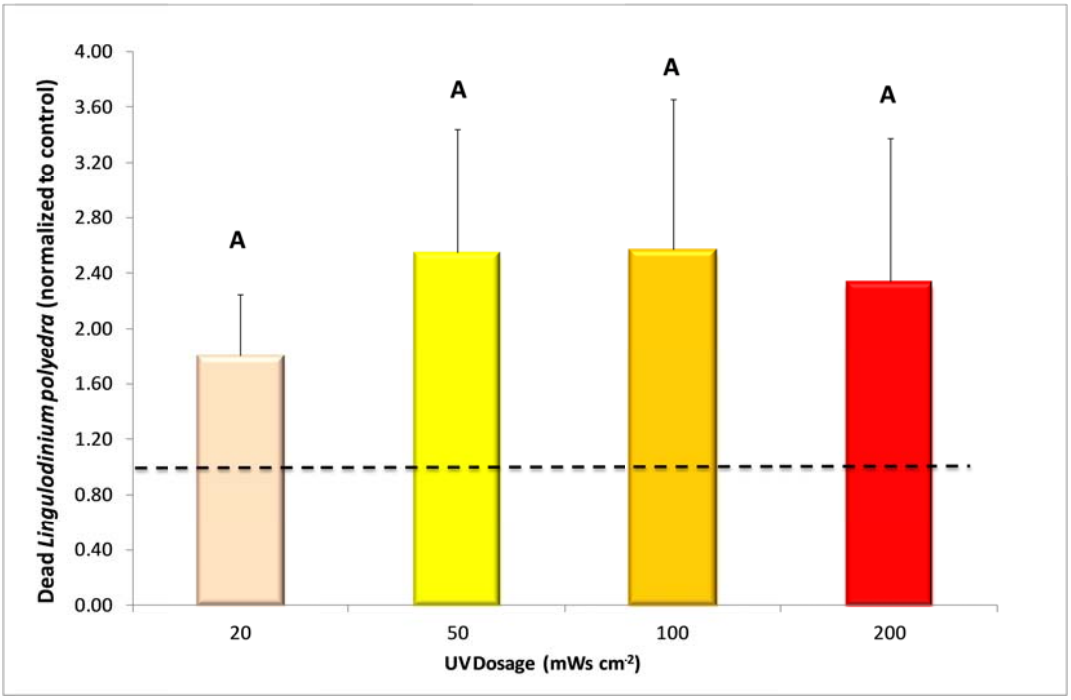

Figure 24: Normalized dead concentrations of *L. polyedra* of each UV treatment using the UV collimated beam. The bars show the normalized mean of the five manual epifluorescence microscopy analytical replicates (Day 0, Day 1, Day 3, Day 5, and Day 10) and the dotted line marks equal concentration to the control. The letters represent significant differences (ANOVA, $p > 0.05$).

The dead concentrations of *L. polyedra* of each treated sample normalized to the control (normalized = treated/control) are presented in Figure 24. Because the concentration of dead *L. polyedra* were higher in the treated samples than in the control sample, the values are above the dotted line, which marks the concentration equal to the control (1.00). There was no significant difference between the normalized treated samples of the dead concentration of *L. polyedra* (ANOVA, $p = 0.707$). Dead organisms were roughly 2 fold more concentrated than living cells, indicating the efficacy of UV treatment.

2.3. *L. polyedra* cysts - Manual epifluorescence Microscopy

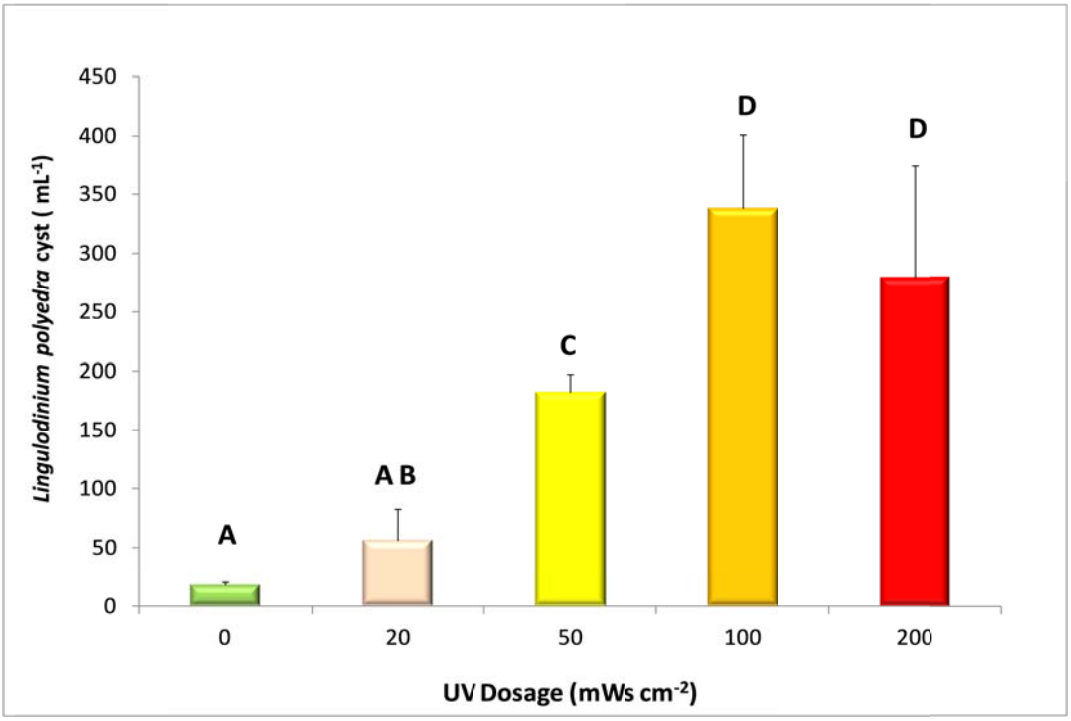

Figure 25: Concentration *L. polyedra* cysts (cysts mL^{-1}) determined by epifluorescence microscopy for each UV treatment using the UV collimated beam. The letters represent significant differences and the bars show the mean concentration (± 1 SD) of 3 replicates over five set analysis set time periods (Day 0, Day 1, Day 3, Day 5, and Day 10) (ANOVA, $p > 0.05$).

There is no significant difference in cyst concentration between the control and the samples treated at 20 mWs cm^{-2} (ANOVA, $p = 0.389$) as shown in Figure 25. However, there was a significant increase in cyst concentration in samples treated at 20 mWs cm^{-2} (57 ± 27 cysts mL^{-1}) to samples treated at 50 mWs cm^{-2} (182 ± 16 cysts mL^{-1}). The concentration significantly increased from the samples treated at 50 mWs cm^{-2} to 100 mWs cm^{-2} (337 ± 64 cysts mL^{-1}). Between the 100 and 200 mWs cm^{-2} treated samples, there was no significant difference in concentrations of *L. polyedra* cysts (ANOVA, $p = 0.209$).

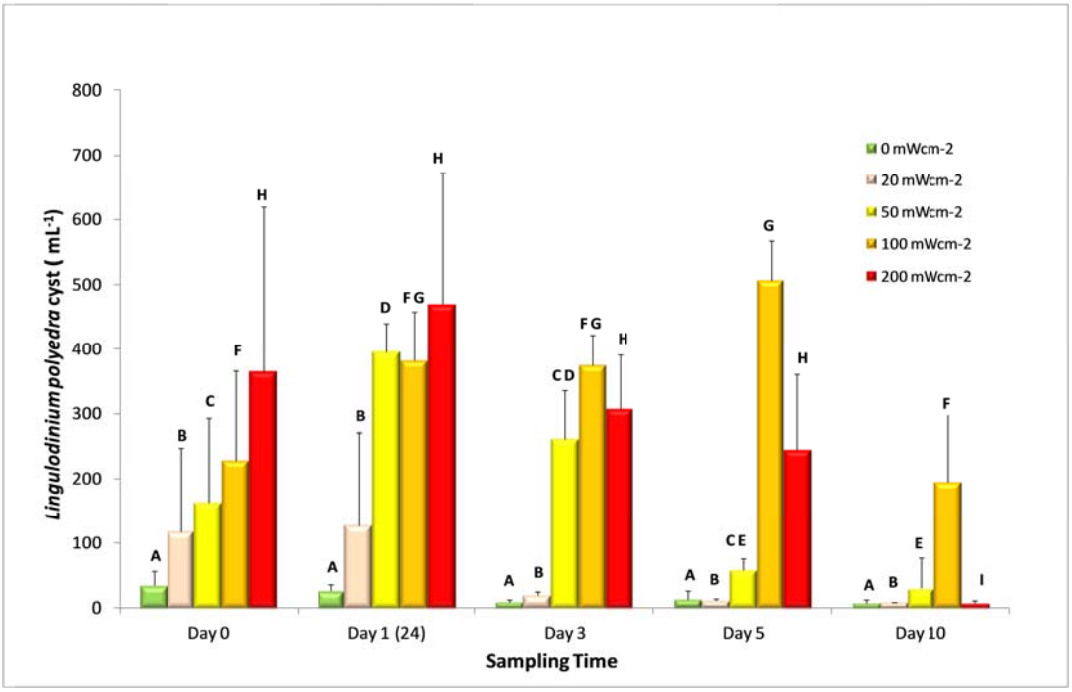

Figure 26: Concentration of *L. polyedra* cysts (cysts mL^{-1}) at multiple UV treatments using the collimated beam over the epifluorescence microscopy sample analysis time period. The bars show the mean concentration (± 1 SD) of 3 replicates for each treatment over time. The letters represent significant differences among sample (ANOVA, $p > 0.05$).

The concentration of cysts in the control (ANOVA, $p = 1.116$) and samples treated at 20 mWs cm^{-2} (ANOVA, $p = 0.286$) did not significantly change over the entire sample analysis time period of the collimated beam trials (Figure 26). The concentration of *L. polyedra* cysts treated at 50 mWs cm^{-2} increased from Day 0 (164 ± 130 cysts mL^{-1}) to Day 1(395 ± 45 cysts mL^{-1}) and then significantly decreased from Day 3 (261 ± 75 cysts mL^{-1}) to Day 5 (58 ± 18 cysts mL^{-1}). Observing the cyst concentration in samples treated at 100 mWs cm^{-2}, concentrations gradually increased over the analysis time period and increased significantly from Day 0 (229 ± 138 cysts mL^{-1}) to Day 5 (506 ± 61 cysts mL^{-1}). There was no significant difference in the *L. polyedra* cyst concentrations in the samples treated at 200 mWs cm^{-2} until significantly decreased from Day 5 (245 ± 116 cysts mL^{-1}) to Day 10 (7 ± 5 cysts mL^{-1}).

2.4. PAM Fluorometry - Photochemical Yield (*Y*)

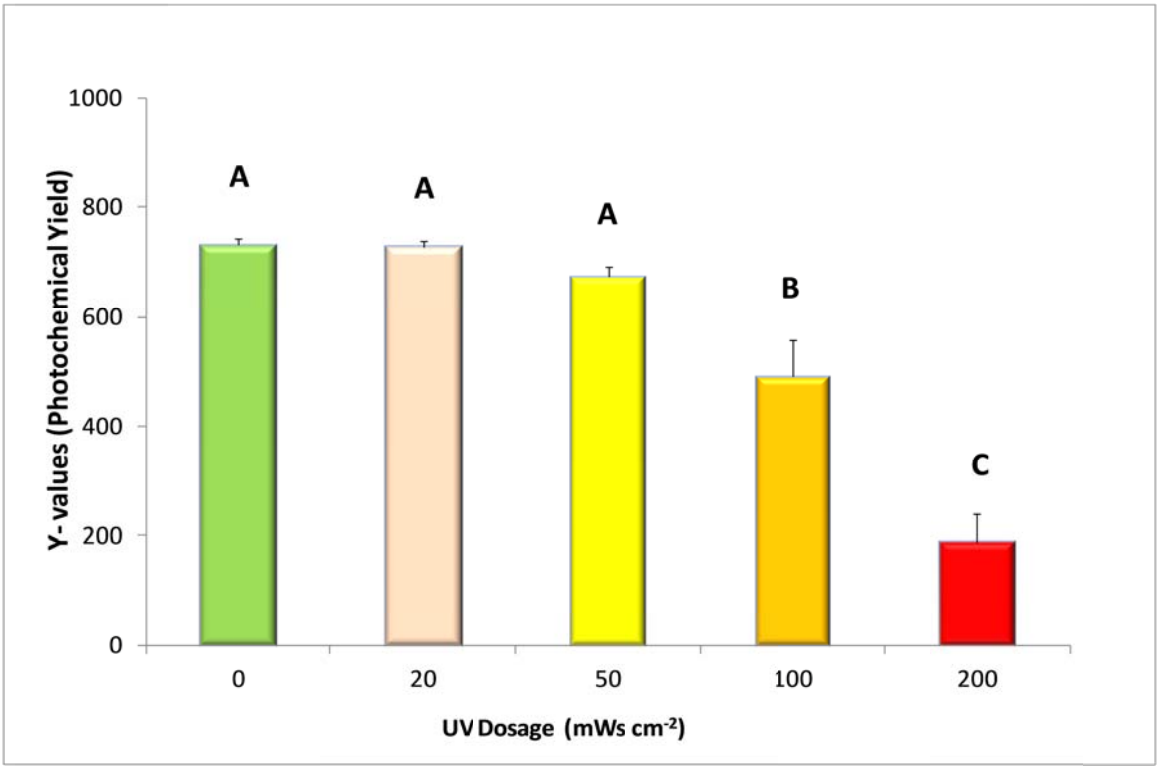

Figure 27: The photochemical yield (*Y*) of *L. polyedra* determined by PAM fluorometry for each UV treatment using the UV collimated beam. The letters represent significant differences and the bars show the mean concentration (± 1 SD) of 3 replicates over three set analysis time periods (Day 0, Day 1, Day 3, Day 5, and Day 10).

Presented in Figure 27, there was no significant difference in the photochemical yield between the control and the *L. polyedra* samples treated at 20 and 50 mWs cm^{-2} (ANOVA, $p > 0.05$). There was a significant decrease the photochemical yield for samples treated at 50 mWs cm^{-2} (674 ± 19 *Y* value) and 100 mWs cm^{-2} (490 ± 68 *Y* value). Again, there was a significant decrease from the 100 mWs cm^{-2} to the 200 mWs cm^{-2} (188 ± 52 *Y* value).

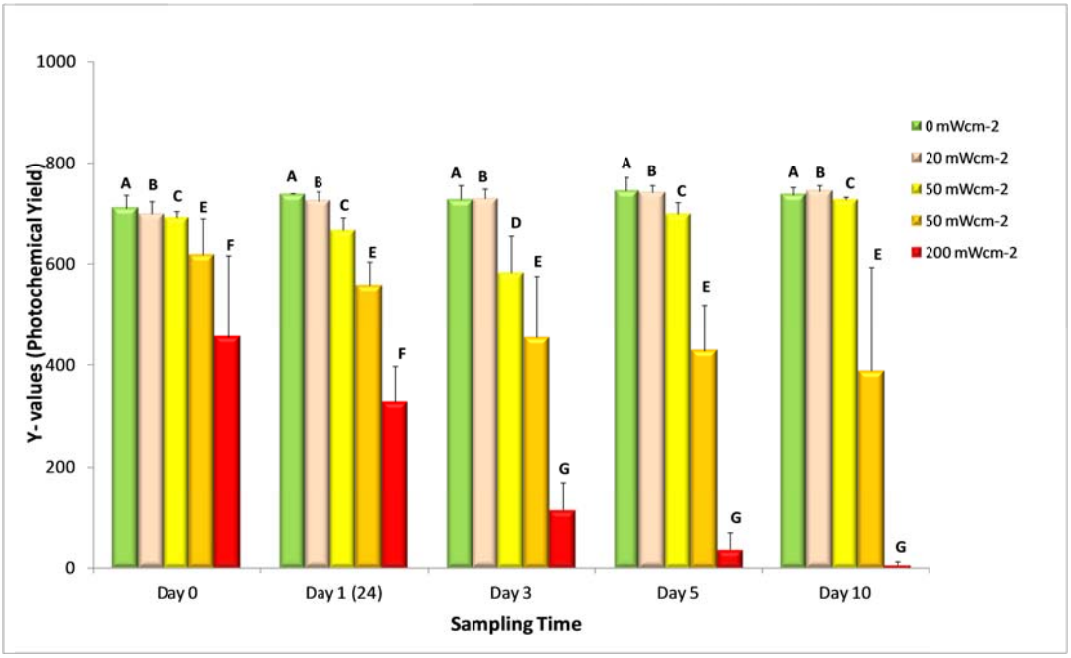

Figure 28: The photochemical yield (Y) of *L. polyedra* samples determined by PAM fluorometry over the sample analysis time. The bars show the mean concentration (± 1 SD) of 3 replicates for each treatment over time. The letters represent significant differences (ANOVA, $p > 0.05$)

There was no significant change in the photochemical yield in the control, and *L. polyedra* samples treated at 20 and 100 mWs cm^{-2} over the sample analysis time period as seen in Figure 28. The photochemical yield of samples treated at 50 mWs cm^{-2} decrease from Day 1 (667 ± 25 *Y* value) to Day 3 (583 ± 73), but stabilized at Day 5 and Day 10. There was no significant change in photochemical yield in *L. polyedra* samples treated at 200 mWs cm^{-2} at Day 0 (456 ± 161 *Y* value) and Day 1 (329 ± 69 *Y* value) but significantly decrease at Day 3 (114 ± 56).

VI. Discussion

1. UV treatment of Live *Lingulodinium polyedra*

The present results show that a consistent and exact measureable UV treatment above 100 mWs cm^{-2} decreases a living concentration of *Lingulodinium polyedra* when viability is measured by manual epifluorescence with associated viability stains (FDA/CMFDA). This is also true when measuring the photochemical yield using a highly sensitive PAM fluorometer. The results show that a UV dose above 100 mWs cm^{-2} will decrease live concentrations while increasing dead concentrations of *L. polyedra* measured by manual epifluorescence microscopy. The physiological state of the organism did not decrease until samples were treated at 100 mWs cm^{-2} when measuring viability using the PAM fluorometer. This occurred in both the UV crosslinker trials as

well as the collimated beam trials. The results also show a decrease in live concentration of *L. polyedra* over time when treated above 100 mWs cm^{-2} particular after 5 days. There were no identified live *L. polyedra* concentrations in 200 mWs cm^{-2} treated samples after 10 days when samples were analyzed by manual epifluorescence microscopy. The photo-chemical yield results at 10 days following UV treatment of 200 mWs cm^{-2} was also below a *Y* value of 250, indicating chlorophyll a fluorescence originating from dead or moribund cells.

2. *Lingulodinium polyedra* cyst concentrations following UV treatment

A UV treatment as low as 50 mWs cm^{-2} will induce cells of *Lingulodinium polyedra* to encyst. The concentration of cysts also increased overtime for treated samples at 50, 100, 200, 300, and 500 mWs cm^{-2}. In regards to the collimated beam trials, the cyst concentrations decreased at 10 days for the 100 and 200 mWs cm^{-2} treated samples, which likely indicates that these enumerated cysts were not viable. Additionally, the live concentrations did not increase at Days 3, 5, or Day 10 of the collimated beam trials, which assumes that excystment, did not occur.

To further assess this anomaly and determine if UV treatment induces cysts and that these cysts are viable, additional methods to measure viability are suggested (e.g., Most Probable Number [MPN] and cyst isolation). In addition to manual epifluorescence microscopy and PAM fluorometry methods, an MPN technique using initial high concentrations of *L.polyedra* prior to treatment could provide a further indication if cells are inactivate and unable to replicate. Monitoring isolated cysts in sterile medium in optimal conditions over an extended period of time (i.e., weeks) could assist in determine if the induce cysts are viable. This will be identified by excystment of live cells from the isolated cyst.

3. Shipping Industry and Technology Vendors

Due to the presented results in this document, it is suggested that detail be accounted for in the design and specifications of a UV treatment technology employed on BWMS. The system should provide an exact and measureable UV dose at a minimum of 100 mWs cm^{-2} treating the entire water column. Numerous factors will contribute to acquiring this exact/known dose, which include flow rate (e.g. exposure time), pipe diameter (e.g. water depth) and continuous flow (e.g. mixing). The technology will also have to be adaptable to accommodate for differences in parameters (e.g. pipe diameter, etc.) found among vessels.

UV treatment technologies need to be vigorously tested following the ETV and IMO land-based testing protocols as well as shipboard protocols prior to being installed and used aboard a functioning ship. Test facilities should measure the viability signal using a variety of techniques to accredit the possible differences in organism response

among organisms, as some organisms may respond differently from others. It is also suggested that national and international facilities as well academia should examine the response of other HABs and red tide forming organisms (*Karenia brevis*) in their experimental approach. Experiments should include standard cell concentrations (~1000 mL^{-1}) as well as blooming concentrations (100,000 – 1,000,000 mL^{-1}) as the response may be different. Currently, ballast water test facilities only examine indigenous assemblages in different size classes and their response to treatment with BWMS. HABs and red tides should be included in this matrix to further assess the efficacy of a technology.

VII. Conclusions

When viability was measured using epifluorescence microscopy with associated viability stains (FDA/CMFDA), samples treated at 100 mWs cm^{-2} decreased living concentrations of *Lingulodinium polyedra* rejecting the null hypothesis. When samples of *L. polyedra* were treated above 100 mWs cm^{-2}, dead concentrations increased as the live concentrations decreased over time.

When viability was measured using PAM fluorometry, physiological state of the organism decreased when samples were treated at 100 mWs cm^{-2}. The photochemical yield for samples treated at 200 mWs cm^{-2} drop below a *Y* value of 300 following a 5 day and 10 day hold times.

VIII. References

Alonso-Rodriguez R., and F. Paez-Osuna. "Nutrients, phytoplankton and harmful algal blooms in shrinp ponds: A review with special reference to the situation in the Gulf of California." *Aquaculture*, 2003: 317-336.

Anderson, D.M. "Turning back the harmful red tide." *Nature*, 1997: 513-514.

Anderson, Kokinos J. P. and D.M. "Morphological Development of Resting Cysts in Cultures of Marine Dinoflagellate Lingulodinium polyedrum (=L. Machaerophorum)." *Palynology*, 1995: 143-166.

Anderson., Pfiester L.A. and D.M. "Dinoflagellate reproduction." *The biology of dinoflagellates*, 1987: 611–648.

B., Poggeler. "Pineal Hormone Melatonin Oscillates Also in the Dinoflagellate Gonyaulax polyedra." *Naturwissenschaften*, 1991: 268- 269.

Backer .LC., Fleming L.E., Rowan, A., Cheng, Y.S., Benson J., Pierce R.H., Zaias J., Bean j, Bossart G.D., Johnson D., Quimbo, R. "Recreational exposure to aerosolized brevetoxins during Florida red tide events." *Harmful Algae*, 2003: 19–28.

Balzer, Ivonne. "Encystment of Gonyaulax polyedra: Dependence on Light." *Biological Rhythm Research*, 1996: 386-389.

Berman J.M., Arrigo K.R., and P.A. Matson. "Agricultrual runoff fuels large plankton blooms in vulnerable areas of the ocean." *Nature*, 2005: 434:211- 214.

Camacho F.G., Rodriguez J.G., Miron A.S., Garcia M.C.C., Belarbi E.H., Chisti Y. and E.M. Grima. "Biotechnological significance of toxic marine dinoflagellates." *Biotechnology Advances*, 2007: 176–194.

Cloren, J. E., and R. Dufford. "Phytoplankton community ecology: Principles applied in San Francisco Bay." *Marine Ecology Progress Series*, 2005: 11-28.

Diamadopoulos, Tsolaki E. and E. "Technologies for ballast water treatment: a review ." *Journal of Chemical Technology and Biotechnology*, 2010: 19-32.

Hardeland, Balzer I. and R. "Photoperiodism and Effects of Indoleamines in a Unicellular Alga, Gonyaulax polyedra." *Reports*, 1991: 795-797.

Ho., Lam C.W.Y. and K.C. "Red tides in Tolo Harbour, Hong Kong." *Red tides: biology,environmental science and toxicology*, 1989: 49-52.

Lennert-Cody, C. E., and P. J. S. Franks. "Plankton patchiness in high-frequency internal waves." *Marine Ecology Progress Series*, 1999: 59–66.

Lewis, J. and R. Hallet. "Lingulodinium polyedrum (Gonyaulax polyedra)—a blooming dinoflagellate." *Oceanography Marine Biology*, 1997: 97–161.

Omand M.M., LeichterJ.J., Franks P.J.S., Guza R.T., Lucas A.J., and F. Federsen. "Physical and biological processes underlying the sudden surface appearance of a red tide in the nearshore." *Journal of Limnology Oceanography*, 2011: 787–801.

Organization, International Maritime. *International Convention for the Control and Management of Ships' Ballast Water and Sediments, 2004'.* Convention BWM/CONF/36, 2004.

Organization, International Maritime. "International Convention for the Control and Management of Ships' Ballast Water and Sediments, 2004'." *Convention BWM/CONF/36* (Convention BWM/CONF/36), 2004.

Organization, International Maritime. "International Convention for the Control and Management of Ships' Ballast Water and Sediments, 2004'." *Convention BWM/CONF/36*, 2004.

Register, U.S. Federal. *Standards for Living Organisms in Ships' Ballast Water Discharged in U.S. Waters; Draft Programmatic Environmental Impact Statement, Proposed Rule and Notice, 74 FR 44631-44672.* Washington, DC: National Archives and Records Administration, 2009.

Steinber M.K., Lemieux E.J. and L.A. Drake. "Determining the viability of marine protists using a combination of vital stains, fluorescent stains." *Marine Biology*, 2011: 1-7.

Takizawa., Yasumoto T. and A. "Fluorometric measuremen tof yessotoxins in shellfi sh by high-pressure liquid chromatography." *Bioscience, Biotechnology, Biochemistry*, 1997: 1775-1777.

Whitehead, M. Vernet and K. "Release of ultraviolet-absorbing compounds by the red-tide dinoflagellate t.ingulodinium polyedra." *Marine Biology*, 1996: 35-44.

IX. Appendices

Appendix A – UV conversion µJ cm^{-2} to mW cm^{-2}

Because UVX the radiometer measures in $mWcm^{-2}$, intensity conversions were needed to determine if the fluence treatment of the crosslinker (displayed in µJ cm^{-2}) was at the desired levels prior to treatment. The follow conversions were used below.

$$Intensity\ (mWcm^{-2}) = Energy\ (mJcm^{-2)})/Time\ (seconds)$$

$$Intensity\ (\mu Wcm^{-2}) = Energy\ (\mu Jcm^{-2})/Time\ (seconds)$$

$$Energy\ (mJcm^{-2}) = \ Intensity\ (mWcm^{-2})\ X\ Time\ (seconds)$$

Example:

$$1{,}000\ mJcm^{-2} = 1\ Jcm^{-2}$$

$$1{,}000\ mWcm^{-2} = 1\ Wcm^{-)}$$

Appendix B – Collimated beam correction factors – Excel Spreadsheet

Table 3 shows the Excel spreadsheet used to integrate the correction factors to determine an exact and measureable incident irradiation/fluence using the UV collimated beam.

Table 3: Excel spreadsheet used to incorporated correction factors to attain exact fluence using the UV collimated beam.

Correction Factors	
Petri Factor	
Petri dish diameter (cm)	5.6
Petri dish area (cm^2)	24.63
Each cm is equal to (in mL)	24.63009
Target volume (mL)	25
Height (cm)	1.015019
Reflectance Factor	0.975
Absorption	
% Transmittance	95
Absorption Coefficient	0.022276
Path length (cm)	1.015019
Total absorbance	0.022611
Water Quality Factor	
Total Absorbance (A)	0.022611
Water Quality Factor	0.974414
Divergent Factor	
Length from surface to light (cm)	33
Sample Pathlength (cm)	1.015019
Divergence	0.97016
True irradiance	
Reading at the center (mW)	2.20E+02
Petri factor	0.95
True irradiance (Ti)	2.09E+02
Germicidal irradiance	
True irradiance (Ti)	209.00000
Reflectance Factor	0.98
Water Quality Factor	0.97
Divergence Factor	0.97
Germicidal irradiance (Gi)	192.64

Appendix C – Data Sheets

During UV treatment of samples of *Lingulodinium polyedra* using the UV crosslinker and UV collimated beam, all necessary parameters were recorded. See data sheets below (Figure 29 Figure 30). Live, dead and cyst counts when conducting the epifluorescence microscopy analysis were recorded on individual data sheets for each sample type (Figure 31).

Figure 29: Data sheet used for the UV crosslinker trials.

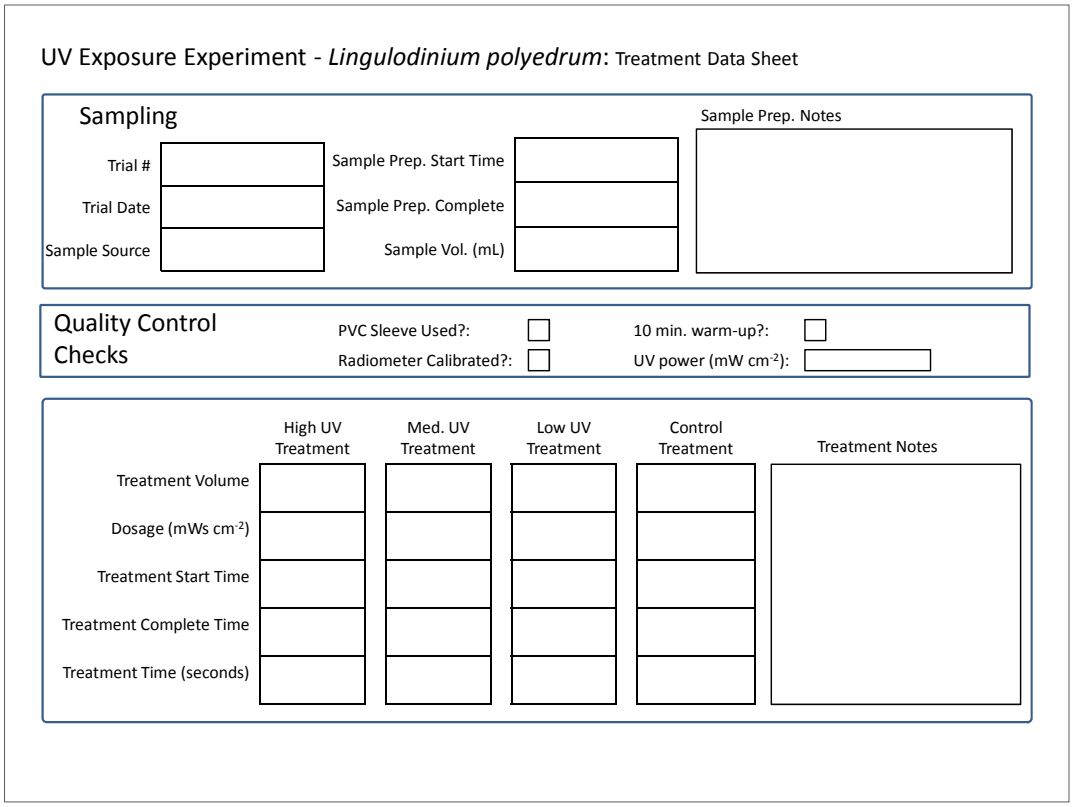

Figure 30: Data sheet used for the UV collimated beam trials.

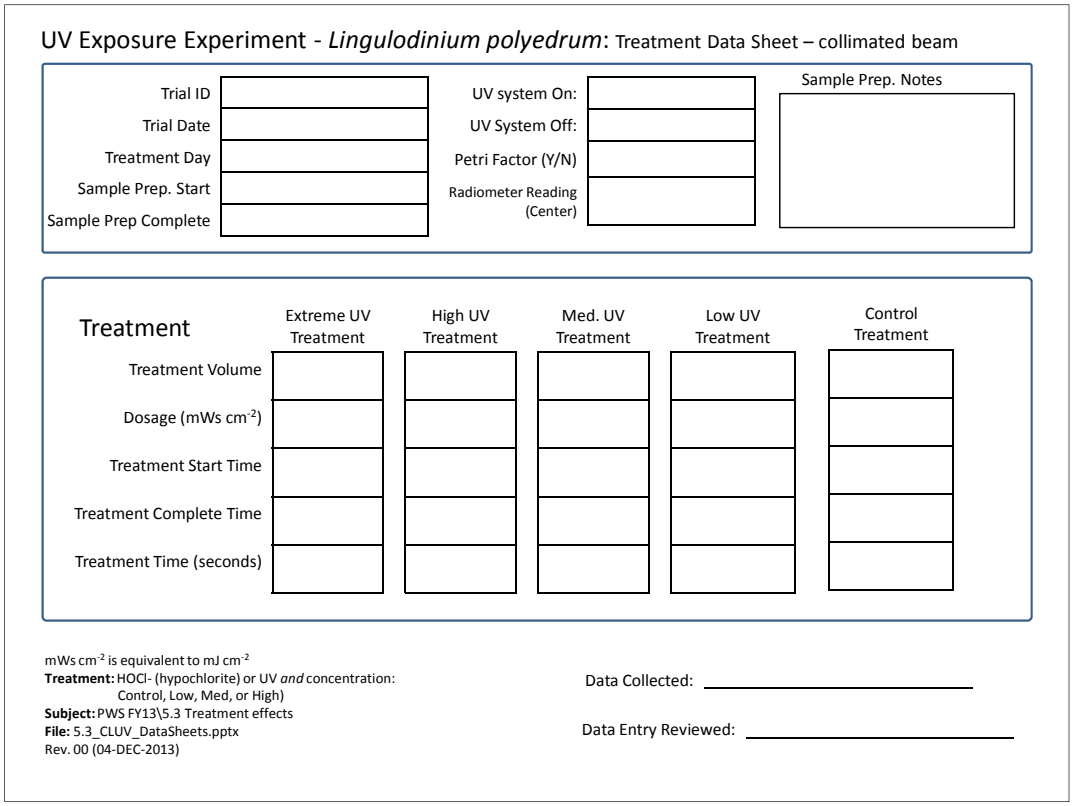

UV Exposure Experiment - *Lingulodinium polyedrum*: Treatment Data Sheet – collimated beam

Trial ID		UV system On:		Sample Prep. Notes
Trial Date		UV System Off:		
Treatment Day		Petri Factor (Y/N)		
Sample Prep. Start		Radiometer Reading (Center)		
Sample Prep Complete				

Treatment	Extreme UV Treatment	High UV Treatment	Med. UV Treatment	Low UV Treatment	Control Treatment
Treatment Volume					
Dosage (mWs cm^{-2})					
Treatment Start Time					
Treatment Complete Time					
Treatment Time (seconds)					

mWs cm^{-2} is equivalent to mJ cm^{-2}
Treatment: HOCl- (hypochlorite) or UV *and* concentration: Control, Low, Med, or High)
Subject: PWS FY13\5.3 Treatment effects
File: 5.3_CLUV_DataSheets.pptx
Rev. 00 (04-DEC-2013)

Data Collected: _____

Data Entry Reviewed: _____

Figure 31: Data sheet used when perform the manual epifluorescence microscopy analysis.

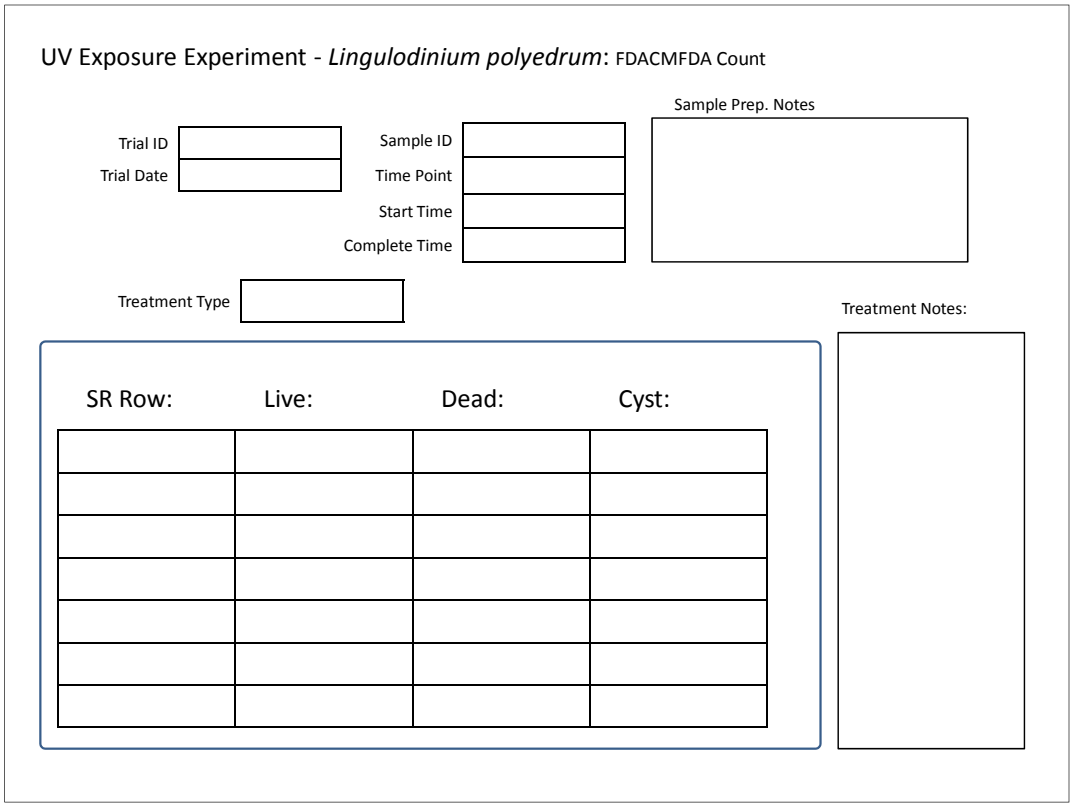

Appendix D – Random Number Generator

Random row order assignments were created using spreadsheet software with a random number generator (Microsoft Excel 2007, Microsoft, Redfield, WA). The examples in this section are specific to Excel.

- Generating Random Numbers

A table of random numbers was generated by using the Excel function, rand(). The number of columns (*n*) was determined by the number of SR counting slide (each column will yield row assignments for SR slide). There should be exactly 20 rows in the table and all of the cells should have the following: = rand(). A secondary table was created with n columns and 20 rows (Table 4, random numbers).

- Ranking the Rows to Determine Counting Order

Once a series of random numbers was generated, a ranking function was used to determine the counting order. The Microsoft Excel spreadsheet includes the ranking function, rank (r1c1, range), where r1c1 is the row number and column number and range is the data range (Table 4, Ranked Row Order). In the table below, the data range is r1:r20 in column 1.

Table 4: Example table generated in Microsoft Excel demonstrating the routine for generating random row counting orders. The first two rows in the first column (Slide 1) show the Excel formula.

Random numbers (each slide = 20)			**Ranked Row Order**			
Slide 1	**Slide 2**	**Slide 3**	**Counting Order**	**Row No. Slide 1**	**Row No. Slide 2**	**Row No. Slide 3**
=rand()	0.76	0.15	1st	***=rank(r1c1, range)***	3	14
=rand()	0.96	0.24	2nd	***=rank(r2c1, range)***	1	11
0.45	0.22	0.39	3rd	10	17	9
0.90	0.75	0.09	4th	4	4	18
0.66	0.71	0.13	5th	7	6	16
0.19	0.21	0.18	6th	17	18	13
0.96	0.28	0.44	6th	2	13	6
0.97	0.43	0.27	8th	1	10	10
0.26	0.61	0.14	9th	15	8	15
0.26	0.22	0.39	10th	14	16	8
0.61	0.30	0.18	11th	8	12	12
0.40	0.24	0.80	12th	12	15	1
0.09	0.74	0.68	13th	19	5	2
0.74	0.27	0.60	14th	5	14	3
0.14	0.01	0.09	15th	18	20	17
0.68	0.50	0.48	16th	6	9	5
0.43	0.62	0.03	17th	11	7	19
0.22	0.42	0.00	18th	16	11	20
0.94	0.81	0.40	19th	3	2	7
0.36	0.16	0.60	20th	13	19	4